JOURNAL OF GEOPHYSICAL RESEARCH, VOL. 101, NO. D13, PAGES 18,835–18,859, AUGUST 20, 1996

Chlorine deactivation in the lower stratospheric polar regions during late winter: Results from UARS

M. L. Santee,[1] L. Froidevaux,[1] G. L. Manney,[1] W. G. Read,[1] J. W. Waters,[1] M. P. Chipperfield,[2] A. E. Roche,[3] J. B. Kumer,[3] J. L. Mergenthaler,[3] and J. M. Russell III[4]

Abstract. Recovery from enhanced chlorine conditions in the lower stratospheric polar regions of both hemispheres is investigated using data from the Upper Atmosphere Research Satellite (UARS). Microwave Limb Sounder (MLS) measurements of ClO within the polar vortices are used to infer ClO_x ($ClO+2Cl_2O_2$) abundances that are then correlated with simultaneous Cryogenic Limb Array Etalon Spectrometer (CLAES) measurements of $ClONO_2$ and Halogen Occultation Experiment (HALOE) measurements of HCl obtained starting within 5 days of the end of the MLS and CLAES high-latitude observing periods in each hemisphere. Time series of vortex-averaged mixing ratios are calculated on two potential temperature surfaces (585 K and 465 K) in the lower stratosphere for approximately month-long intervals during late winter: August 17 – September 17, 1992, in the southern hemisphere and February 12 – March 16, 1993, in the northern hemisphere. The observed mixing ratios are adjusted for the effects of vertical transport using diabatic vertical velocities estimated from CLAES tracer data. In the northern hemisphere, the decrease in ClO_x is balanced on both surfaces by an increase in $ClONO_2$. In the southern hemisphere, continuing polar stratospheric cloud activity prevents ClO from undergoing sustained decline until about September 3. In contrast to the northern hemisphere, there is no significant chemical change in vortex-averaged $ClONO_2$ at 465 K, and there is an apparent decrease in $ClONO_2$ at 585 K, even after the enhanced ClO abundances have started to recede. Results from the SLIMCAT chemical transport model [*Chipperfield et al.*, this issue] initialized with UARS data and run with $OH + ClO \rightarrow HCl + O_2$ as an 8% channel suggest that the primary recovery product in the south during this time period is not $ClONO_2$, but HCl. HALOE HCl mixing ratios are extrapolated back to the time of the MLS and CLAES data. At 585 K, the chlorine budget can be made to balance by extrapolating HCl back to a value of 0.6 parts per billion by volume (ppbv) at the beginning of the study period; at 465 K, the contribution from extrapolated HCl is not sufficient to offset the loss in ClO_x, and there is a slight imbalance between the decrease in reactive chlorine and the change in chlorine reservoirs. The difficulty in closing the chlorine budget in the southern hemisphere may arise from complications caused by ongoing activation, incomplete photochemical assumptions, and/or inadequate data quality.

1. Introduction

Chlorine chemistry is now known to be responsible for the severe depletion in lower stratospheric ozone observed during late winter and early spring over Antarctica [e.g., *Solomon*, 1988, 1990; *McElroy and Salawitch*, 1989; *Anderson et al.*, 1991; *Brune et al.*, 1991]. Observed decreases in Arctic lower stratospheric ozone have also been shown to be consistent with chlorine-catalyzed destruction [e.g., *Salawitch et al.*, 1990, 1993; *Schoeberl et al.*, 1990; *Hofmann and Deshler*, 1991; *Traub et al.*, 1994; *Braathen et al.*, 1994; *Müller et al.*, 1994]. Reactive chlorine is produced through heterogeneous processes occurring on the surfaces of polar stratospheric clouds (PSCs), which form in the low temperatures of polar winter. These heterogeneous reactions rapidly convert HCl and $ClONO_2$, the reservoir species where most of the inorganic chlorine in the lower stratosphere resides under nonperturbed condi-

[1]Jet Propulsion Laboratory, California Institute of Technology, Pasadena
[2]Department of Chemistry, University of Cambridge, UK
[3]Lockheed Palo Alto Research Laboratory, Palo Alto, California
[4]NASA Langley Research Center, Hampton, Virginia

Paper number 96JD00580.
0148-0227/96/96JD-00580$09.00

tions [*Kawa et al.*, 1992; *Webster et al.*, 1993; *Dessler et al.*, 1995], to species such as Cl_2 and HOCl that are easily photolyzed. Following exposure of the processed air to sunlight, the dominant daytime chlorine species is ClO. Maintenance of high ClO levels leads to ozone loss through a catalytic cycle involving ClO dimer (Cl_2O_2) formation [*Molina and Molina*, 1987].

The timescale for recovery from perturbed chlorine conditions in the lower stratosphere is an important topic because the rate at which enhanced ClO abundances recede bears directly on the cumulative ozone loss at high latitudes. One pathway by which reactive chlorine is shifted back to reservoir form is $ClO + NO_2 + M \rightarrow ClONO_2 + M$. In addition to promoting chlorine repartitioning, heterogeneous processes also inhibit reformation of $ClONO_2$ by sequestering reactive nitrogen as HNO_3 in PSC particles. When temperatures rise above the PSC evaporation threshold, gaseous HNO_3 is released; the HNO_3 then photolyzes (on a timescale of ~30 days for a solar zenith angle of 70° [*Kawa et al.*, 1992]) to produce NO_2. If sufficient NO_2 is available, $ClONO_2$ formation takes place in a few hours. Alternatively, chlorine deactivation can proceed via the reaction $Cl + CH_4 \rightarrow HCl + CH_3$. Under non-ozone-depleted conditions, the timescale for HCl reformation is roughly comparable to the timescale for HNO_3 photolysis [*Kawa et al.*, 1992]. However, *Prather and Jaffe* [1990] have shown that very low ozone concentrations lead to a highly nonlinear chemical system in which the conversion of ClO to HCl is substantially accelerated through an increase in the Cl to ClO abundance ratio. *Crutzen et al.* [1992] also saw a rapid increase in modeled HCl during recovery under "ozone hole" conditions. This conversion to HCl when ozone abundances are low has been noted in UARS data by *Douglass et al.* [1995].

Significant interhemispheric differences in the recovery timescale are expected due to underlying differences in seasonal temperature patterns and vortex behavior [e.g., *Andrews et al.*, 1989; *World Meteorological Organization (WMO)*, 1995]. On average, temperatures are ~15–20 K higher, and the vortex is weaker and more distorted, in the Arctic than in the Antarctic, leading to fewer and less persistent PSC events in the Arctic. Denitrification, the removal of nitrogen from the lower stratosphere through gravitational settling of PSC particles containing HNO_3, is much less extensive in the Arctic than in the Antarctic [e.g., *Fahey et al.*, 1989; *Toon et al.*, 1989; *Coffey et al.*, 1989; *Mankin et al.*, 1990; *Kawa et al.*, 1990; *Poole and Pitts*, 1994; *Santee et al.*, 1995]. Although enhanced ClO abundances have been observed in the polar vortices of both hemispheres [*de Zafra et al.*, 1987; *Anderson et al.*, 1989; *Waters et al.*, 1993a, b], the accompanying loss of Arctic ozone has been much less severe [*Hofmann et al.*, 1989; *Evans* 1990; *Hofmann and Deshler*, 1991; *Kyrö et al.*, 1992; *Manney et al.*, 1994a] than that over Antarctica. The warmer temperatures, greater dynamical activity, and continued presence of HNO_3 throughout northern winter moderate ozone loss and prevent the formation of an Arctic ozone "hole" [*Brune et al.*, 1991; *Schoeberl and Hartmann*, 1991; *Santee et al.*, 1995]. Differences in the late winter/early spring HNO_3 and O_3 concentrations between the two hemispheres lead to dissimilarities in the production rates of the chlorine reservoirs.

Chlorine deactivation has been the subject of several previous investigations. *Toohey et al.* [1993] and *Webster et al.* [1993] report simultaneous in situ measurements of ClO and HCl from the second Airborne Arctic Stratospheric Expedition (AASE II) in the 1991–1992 Arctic winter. They find that decreasing ClO abundances during the recovery phase are consistent with the rapid formation of $ClONO_2$ (calculated from an estimate of the total available inorganic chlorine), while HCl remains substantially depleted through the end of the observational period in February 1992. Contemporaneous observational [*Adrian et al.*, 1994; *Oelhaf et al.*, 1994; *Bell et al.*, 1994] and modeling [*Lutman et al.*, 1994; *Müller et al.*, 1994] studies from the European Arctic Stratospheric Ozone Experiment (EASOE) find the same recovery pattern: after cessation of PSC activity, there is an almost complete conversion of active chlorine to $ClONO_2$, which remains the dominant inorganic chlorine compound for more than a month. Similarly, *Blom et al.* [1995] report aircraft observations taken during the 1992–1993 Arctic winter that indicate that most of the inorganic chlorine in the vortex has been converted to $ClONO_2$ by the end of March. These recent findings confirm the conclusions from earlier modeling studies constrained by AASE observations [*Jones et al.*, 1990; *McKenna et al.*, 1990]. Over Antarctica, infrared solar spectra recorded at McMurdo in late winter/early spring 1986 indicate a twofold increase in column HCl + $ClONO_2$ associated with rapidly rising temperatures [*Farmer et al.*, 1987]. While the sum of HCl and $ClONO_2$ remains roughly constant thereafter, the $ClONO_2$/HCl ratio gradually declines from 1.5 in late September to 0.3 in late October. *Liu et al.* [1992] also use HCl column amounts retrieved from infrared solar spectra obtained at McMurdo, in combination with a one-dimensional photochemical model, to show that almost all active chlorine species are converted back to HCl by mid-October. Rapid conversion of ClO to the reservoirs $ClONO_2$ and HCl occurs once PSCs evaporate, followed by slow repartitioning between the reservoirs. *Schoeberl et al.* [1993] perform trajectory analyses of ClO and NO measurements from both Arctic and Antarctic aircraft campaigns and conclude that production of $ClONO_2$ is the main mechanism for the initial decay of high ClO concentrations when the air is not denitrified; in highly denitrified parcels, lack of HNO_3 (and therefore NO_2) prevents transformation of ClO to $ClONO_2$, and ClO remains enhanced.

In this paper we use data from the Upper Atmosphere Research Satellite (UARS) to examine chlorine reservoir recovery in the lower stratospheric polar regions of both hemispheres. Microwave Limb Sounder (MLS) measurements of ClO within the polar vortices are correlated with simultaneous Cryogenic Limb Array Etalon Spectrometer (CLAES) observations of $ClONO_2$ and

Halogen Occultation Experiment (HALOE) observations of HCl obtained shortly after the MLS and CLAES data. We analyze time series of vortex-averaged mixing ratios on two potential temperature surfaces (585 K and 465 K) in the lower stratosphere for approximately month-long intervals during late winter: August 17 – September 17, 1992, in the southern hemisphere and February 12 – March 16, 1993, in the northern hemisphere. We focus on the late-winter balance between the decay of reactive chlorine and the growth of chlorine reservoir species based on these data sets, and we compare the observational results with those from the SLIMCAT chemical transport model [see *Chipperfield et al.*, this issue] initialized with UARS data.

2. Data and Instrument Description

MLS acquires millimeter-wavelength thermal emission measurements that are not degraded by PSCs or aerosol. The measurement technique and the instrument are described in detail by *Waters* [1993] and *Barath et al.* [1993], respectively. MLS observations of stratospheric ClO have been presented previously by *Waters et al.* [1993a, b, 1995] and *Manney et al.* [1994a]. The estimated precision (rms) and absolute accuracy of an individual ClO profile in the lower stratosphere are ~0.5 parts per billion by volume (ppbv) and 15–20%, respectively [*Waters et al.*, 1996] for Version 3 files. *Waters et al.* [1996] report a bias error in the Version 3 ClO data due to HNO_3, which has a small effect on the ClO signal but which is accounted for only by assuming climatological values. When HNO_3 abundances depart substantially from climatology (e.g., under conditions of severe denitrification in the Antarctic vortex), Version 3 ClO values are too large by ~0.1 ppbv at 22 hPa and ~0.2 ppbv at 46 hPa [*Waters et al.*, 1996]. In this study, we utilize ClO values from preliminary algorithms that also retrieve HNO_3, eliminating the bias error in the Version 3 results [*Waters et al.*, 1996] (although it makes little difference in the northern hemisphere, where HNO_3 is not depleted). These ClO data have an accuracy of about 10%. *Waters et al.* [1996] also report a scaling error in the Version 3 ClO data that arises because the ClO line strength factor is 8% greater than the value (erroneously) used in the current retrievals. We account for this error by reducing the retrieved ClO abundances by 8%. Overall, the vortex averages presented below have an estimated precision of ~0.05 ppbv.

CLAES [*Roche et al.*, 1993a] measures infrared thermal emission in nine spectral regions between 3.5 μm and 13 μm. MLS and CLAES observations are essentially simultaneous and colocated (typically to within a few tens of kilometers). CLAES $ClONO_2$ measurements have been reported by *Roche et al.* [1993b, 1994]; here we use Version 7 files, which have an estimated systematic error of less than 20% and a single-profile precision of ~0.2 ppbv in the lower stratosphere [*Mergenthaler et al.*, 1996]. To eliminate spikes and other known artifacts in the data, all points for which the $ClONO_2$ value either exceeds 3.5 ppbv or exceeds 1.5 ppbv with an associated error of greater than 50% are excluded from the analysis [*Mergenthaler et al.*, 1996]. We also utilize CLAES observations of the dynamical tracers CH_4 and N_2O [*Kumer et al.*, 1993; *Roche et al.*, 1996]. For CH_4 the estimated systematic error and precision are about 15% and 0.1 parts per million by volume (ppmv), respectively, at 46 hPa, and the mixing ratios are most reliable for values below 1.5 ppmv. For N_2O the estimated systematic error and precision are about 20% and 20 ppbv, respectively, at 46 hPa, and the mixing ratios are most reliable for values below 250 ppbv. In addition to constituent mixing ratios, aerosol extinction coefficients are also retrieved from the measured spectra [*Mergenthaler et al.*, 1993; *Massie et al.*, 1996]. The aerosol data we show here are from the 790 cm^{-1} spectral region, where there is strong spectral contrast between gas (O_3 and CO_2) line emission and aerosol continuum emission.

Both CLAES and MLS are situated on the anti-Sun side of the spacecraft, and both of their optical pointing axes are directed approximately 23° down from the local horizontal at the observation point. This pointing geometry, coupled with the 57° inclination of the UARS orbit, leads to measurement coverage from 80° latitude on one side of the equator to 34° on the other. The UARS orbit plane precesses in such a way that all local solar times are sampled in about 36 days (getting ~20 min earlier each day at a given latitude), after which the spacecraft is rotated 180° about its yaw axis. Thus 10 times per year MLS and CLAES alternate between viewing northern and southern high latitudes.

HALOE uses solar occultation to measure the attenuation of infrared solar energy due to stratospheric constituents [*Russell et al.*, 1993]. In this study we use Version 17 HCl data, which are described by *Russell et al.* [1996]. Because measurements are made only at the spacecraft sunrise and sunset times, daily sampling typically consists of 15 sunrise profiles at one particular latitude and 15 sunset profiles in the opposite hemisphere. The HALOE observing pattern moves slowly north and south throughout the year, with wintertime coverage of the most extreme southern latitudes (nearly to 80°S) occurring from mid-September to mid-October and wintertime coverage of the most extreme northern latitudes (nearly to 80°N) occurring from mid-March to mid-April. In the 1992 southern and 1992–1993 northern late-winter periods, HALOE measurements are not obtained within the polar vortices until after the spacecraft has yawed toward the opposite hemisphere; thus these HALOE high-latitude data are not contemporaneous with either the MLS or the CLAES data.

3. 1992 Southern Hemisphere Winter

3.1. Behavior of ClO and $ClONO_2$

As discussed in section 1, high levels of vortex ClO follow from the heterogeneous activation of chlorine as temperatures fall below the PSC existence threshold

(~195 K [*Turco et al.*, 1989]) in early winter. Elevated levels (mixing ratios greater than 1 ppbv) of lower stratospheric ClO were observed in portions of the southern polar vortex as early as June 2 (the beginning of an MLS south-viewing period) [*Waters et al.*, 1993a, b]. ClO abundances continued to increase throughout the winter, and at the start of the next south-viewing period on August 17, 1992, MLS measured lower stratospheric ClO values of about 2 ppbv in most of the sunlit area poleward of 60°S [*Waters et al.*, 1993a, b]. It is for this late-winter (August 17 – September 17, 1992) yaw period that we will examine the relationship between the decrease in ClO and the changes in the reservoir species $ClONO_2$ and HCl.

The behavior of MLS ClO on three selected days at the beginning, middle, and end of the southern hemisphere late-winter observing period is shown in Plate 1a. The data have been interpolated onto constant potential temperature (Θ) surfaces at 585 K (corresponding to ~24 km, 20 hPa for the cold temperatures characteristic of the polar vortex) and 465 K (~19 km, 50 hPa) using U.S. National Meteorological Center (NMC) temperatures. Only data from the "day" side of the orbit are shown because ClO abundances drop sharply in regions where the solar zenith angle (Plate 1b) is greater than ~94°, due to lack of Cl_2O_2 photolysis. Superimposed on each of the maps are three contours of potential vorticity (PV), calculated from NMC temperatures and derived winds using the algorithm described by *Manney and Zurek* [1993]. These PV contours are used to delimit different areas over which averaged mixing ratios are calculated. The outermost contour represents a typical definition of the vortex edge during winter and coincides with a strong barrier to mixing [*Manney et al.*, 1994b]. The innermost contour on each Θ surface has a PV value twice that of the outermost one. The intermediate contour is situated poleward of the vortex boundary; using it reduces the potential impact of horizontal transport from lower latitudes on the averaged mixing ratios and avoids complications associated with the variability and lack of correlation with PV of ClO (and $ClONO_2$) found for the (northern hemisphere) vortex edge region by *Chipperfield et al.* [1995]. Furthermore, this contour more closely delineates the region of high ClO at 465 K in mid-August, and it also closely approximates the edge of the region of low values of N_2O and CH_4 (not shown) caused by strong unmixed diabatic descent within the vortex. The PV contours indicate that the vortex is relatively symmetric with respect to the pole throughout this period, and its size, shape, and strength are roughly constant at both levels.

From mid-August to mid-September the outside edge of enhanced ClO retreats poleward. Elevated ClO abundances recede more rapidly at 585 K than at 465 K, with the majority of the decrease occurring in the latter half of the period. The area poleward of 52°S in which daytime ClO mixing ratios exceed 1 ppbv, shown in Plate 2, is a diagnostic of the time and altitude dependence of the decay of activated chlorine. The value of 52° is selected to generally encompass the maximum areal extent of the vortex at these levels during this time period while excluding lower latitudes (where ClO is not enhanced). The lower stratospheric minimum values occurring at the beginning of September are artifacts caused by a brief interval in the middle of the yaw period during which there are essentially no daylight measurements due to precession of the orbit. As the slope and spacing of the contours in Plate 2 illustrate, the decline in ClO is more rapid at the higher Θ levels and intensifies at the beginning of September.

In the southern polar region, PSCs typically persist at 18 km until at least mid-to-late September [*McCormick et al.*, 1989; *Poole and Pitts*, 1994]. In 1987, PSCs were present at this level into mid-October [*McCormick et al.*, 1989; *Poole and Pitts*, 1994], and results from ER-2 aircraft flights between August 23 and September 22, 1987, show that ClO mixing ratios at 18 km increased throughout this period [*Brune et al.*, 1989]. *Jones et al.* [1989] use the ER-2 observations from early September 1987 to initialize a photochemical model integrated along air parcel trajectories and find that maintenance of elevated ClO concentrations is very dependent on the frequency and duration of PSC events. In this study we use CLAES measurements of aerosol extinction to assess the possibility of continued chlorine activation during our observational period. The area in which aerosol extinction coefficients in the region poleward of 52°S exceed 1.0×10^{-3} km^{-1} [*Turco et al.*, 1989] is given in Plate 3. At the beginning of the late-winter observing period in mid-August, PSC activity is as extensive as it was during the previous June-July south-looking interval (not shown), and heterogeneous chlorine activation is expected to be ongoing. Maps of aerosol extinction on individual days (also not shown) indicate that, although there are no significant PSC events observed to extend up to the 585 K level after the first few days of September, there continue to be intermittent localized PSC events at 465 K as late as September 15. These episodic PSCs may partially explain the slower decline in ClO at 465 K than at 585 K. Because the focus here is on the deactivation of chlorine, we will limit the study to the latter half of the yaw period (starting on September 3), when PSC activity is subsiding and (as seen in Plate 2) the high ClO abundances are receding.

If the primary reservoir for chlorine during the initial stages of recovery were $ClONO_2$, then production of $ClONO_2$ would parallel the reduction in ClO evident in Plates 1 and 2. Maps of CLAES $ClONO_2$ during the late-winter interval are shown in Plate 4. To ensure that the same air parcels are being considered for both ClO and $ClONO_2$, these maps are also constructed using data from the "day" side of the orbit only. As discussed by *Roche et al.* [1993b, 1994], $ClONO_2$ mixing ratios rise steeply from midlatitudes to form a roughly circumpolar collar of enhanced abundances, with some intrusion of high $ClONO_2$ into the vortex core, where values

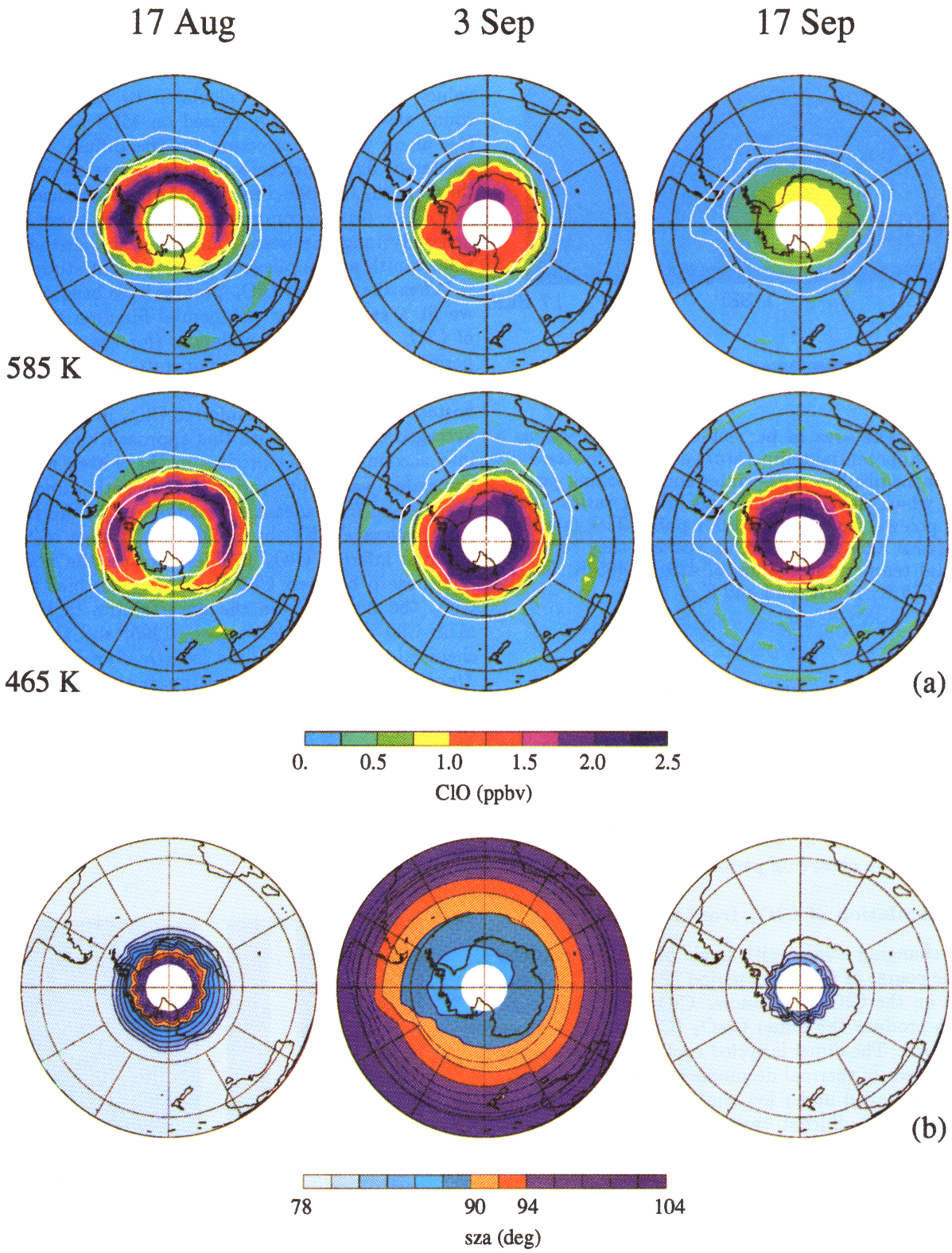

Plate 1. (a) Maps of Microwave Limb Sounder (MLS) ClO for selected days during the 1992 southern hemisphere late-winter south-looking period, interpolated onto the 585 K (top) and 465 K (bottom) potential temperature surfaces using National Meteorological Center (NMC) temperatures. The maps are polar orthographic projections extending to the equator, with the Greenwich meridian at the top and dashed black circles at 30°S and 60°S, and are produced by binning and interpolating measurements taken over a 24-hour period. No measurements were obtained in the white area poleward of 80°S. Only data from the "day" side of the orbit are shown. Superimposed in white on each of the maps are three contours of potential vorticity: -0.70×10^{-4} $Km^2kg^{-1}s^{-1}$, -1.05×10^{-4} $Km^2kg^{-1}s^{-1}$, and -1.40×10^{-4} $Km^2kg^{-1}s^{-1}$ at 585 K, and -0.25×10^{-4} $Km^2kg^{-1}s^{-1}$, -0.375×10^{-4} $Km^2kg^{-1}s^{-1}$, and -0.50×10^{-4} $Km^2kg^{-1}s^{-1}$ at 465 K. (b) Maps of the solar zenith angle (SZA) of the MLS measurements ("day" side of the orbit) for the days shown in Plate 1a. The 94° SZA contour represents the approximate edge of daylight for the measurements.

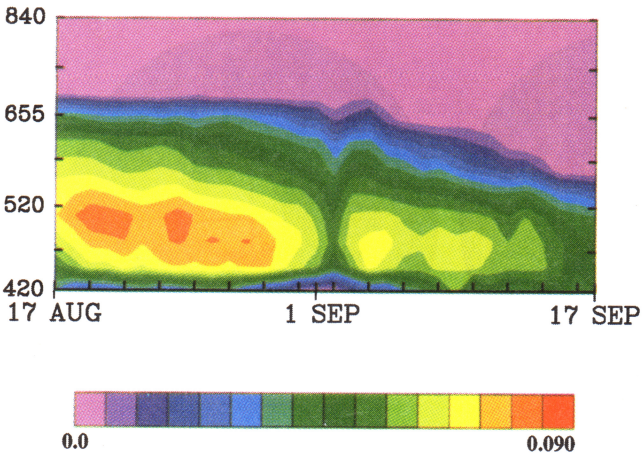

Plate 2. The area in percent of a hemisphere, as a function of potential temperature and time for the 1992 southern hemisphere late-winter south-looking period, within which daytime MLS ClO mixing ratios in the region poleward of 52°S exceed 1 ppbv. Tick marks on the vertical axis are not evenly spaced; they represent potential temperature values of 420 K, 465 K, 520 K, 585 K, 655 K, 740 K, and 840 K.

are generally much smaller than in the collar region. By mid-September the high values of the collar region have diminished at both Θ levels, and an overall increase in $ClONO_2$ comparable to the decrease in ClO is not seen. As shown in Plate 5, the area poleward of 52°S distinguished by high $ClONO_2$ abundances (> 1.5 ppbv) is essentially constant at 465 K but decreases at 585 K throughout the observing period.

3.2. Calculation of ClO_x from MLS ClO

The changing solar zenith angle of the observations over the course of the study period (Plate 1b) has some impact on the ClO abundances. ClO recombines with itself to produce the dimer Cl_2O_2 ($ClO + ClO + M \rightarrow Cl_2O_2 + M$). The dimer is cycled back into ClO through the processes of thermal decomposition and photolysis, which is curtailed under low-sunlight conditions. Thus the pronounced diurnal cycle in ClO is governed by Cl_2O_2 formation, dissociation, and photolysis. When ClO abundances are large, Cl_2O_2 becomes a significant component of the total reactive chlorine and should not be neglected even under daylight conditions.

Since there are no measurements of Cl_2O_2, its contribution is inferred for each vortex measurement of ClO, assuming photochemical equilibrium between ClO and the dimer, coupled with the equation $[ClO_x] = [ClO] + 2[Cl_2O_2]$ [see, e.g., *Rodriguez et al.*, 1989]. This leads to a quadratic equation for $[ClO_x]$ (also used recently by *MacKenzie et al.* [1996]), which is then solved to give the inferred ClO_x profile. We use the recommended photochemical rate constants and dimer absorption cross sections from *DeMore et al.* [1994] in these calculations. The photolysis rate constant (J value) for the Cl_2O_2 is calculated by taking into account absorption by O_3 (based on MLS profiles) and O_2, along with a correction for the diffuse (multiply scattered) flux. The correction factors are derived from the Caltech/JPL one-dimensional photochemical model (M. Allen, private communication, 1995); these factors generally range between 1 and 2 for the altitudes and solar zenith angles relevant to the present study.

When the inferred ClO_x profiles have been obtained, we fit a second-order polynomial function to the set of ClO_x versus ClO abundances (for the entire study period) on each potential temperature surface. These nonlinear functional relationships are used to produce vortex-averaged values of inferred ClO_x from the vortex-averaged ClO data. With this approach we have taken into account all ClO profiles in the vortex and their associated variability (arising from both atmospheric sources and from measurement noise). We did not calculate average ClO_x by taking the average of the individual inferred ClO_x profiles because the nonlinear relationship between ClO and ClO_x can bias average ClO_x too high. Given the uncertainties in both the MLS ClO data [*Waters et al.*, 1996] and the photochemical rate constant data [see *DeMore et al.*, 1994; *MacKenzie et al.*, 1996], we estimate that the resulting uncertainty in inferred ClO_x is about 25%. However, trends in the averaged results are much less affected by these systematic uncertainties. As will be shown below, the inferred vortex-averaged ClO_x abundances are in excellent agreement with those from the SLIMCAT chemical transport model [*Chipperfield et al.*, this issue].

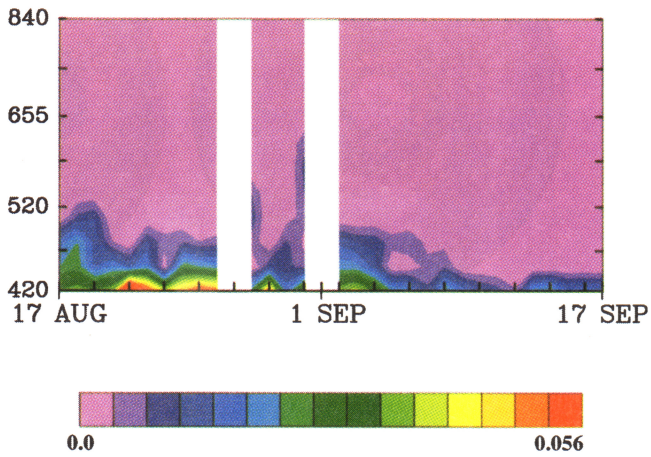

Plate 3. The area in percent of a hemisphere, as a function of potential temperature and time for the 1992 southern hemisphere late-winter south-looking period, within which Cryogenic Limb Array Etalon Spectrometer (CLAES) aerosol extinction coefficients in the region poleward of 52°S exceed 1.0 $\times 10^{-3}$ km^{-1}. Data gaps (white spaces in plots) occur during the implementation of instrument modes other than normal science operations.

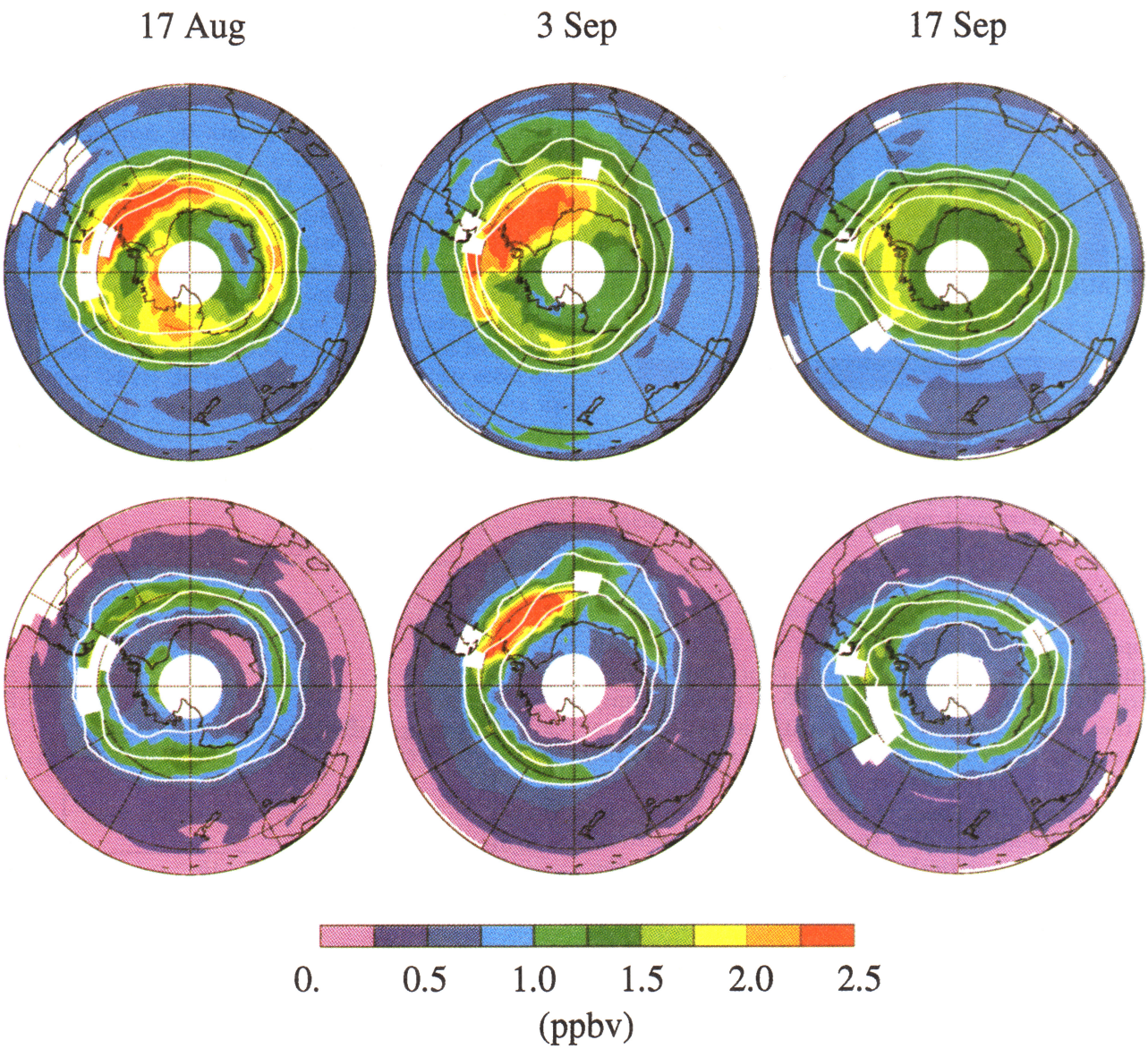

Plate 4. As in Plate 1a (with a different color scale) for CLAES $ClONO_2$. Blank spaces in the maps represent areas where there are data gaps or spurious data points.

3.3. Effects of Vertical Transport

One of the issues that must be addressed in contrasting the behavior of ClO_x and $ClONO_2$ is the possible effect of vertical transport on the mixing ratios at these levels. As the polar regions fall into darkness after the autumnal equinox, radiative processes rapidly cool the polar stratosphere, the vortex spins up, and strong downward motion over this area begins [*Schoeberl and Hartmann*, 1991]. The descending air carries with it the chemical composition of the upper stratosphere; since the vortex edge represents a barrier to horizontal mixing, descent can produce steep mixing ratio gradients across the vortex boundary on an isentropic surface (depending on the vertical profile of the species). Both N_2O and CH_4, which have long chemical lifetimes with tropospheric sources and stratospheric sinks, have been shown to be useful as conservative tracers of stratospheric air motions [e.g., *Loewenstein et al.*, 1989, 1990; *Collins et al.*, 1993].

We estimate the vertical velocities at 585 K and 465 K from CLAES measurements of N_2O and CH_4. Vortex-averaged mixing ratios are calculated by dividing the area integral of the mixing ratio inside a PV contour by the area enclosed by that contour. This calculation is performed for the three PV contours shown in Plate 1a. Similar results are obtained for all PV values; here we discuss the results from the intermediate contour only. Daily vortex-averaged mixing ratios for both N_2O and CH_4 are shown in Figure 1 as a function of time. For perfect tracers in the absence of diabatic descent, the lines fit to the averaged mixing ratios would have zero

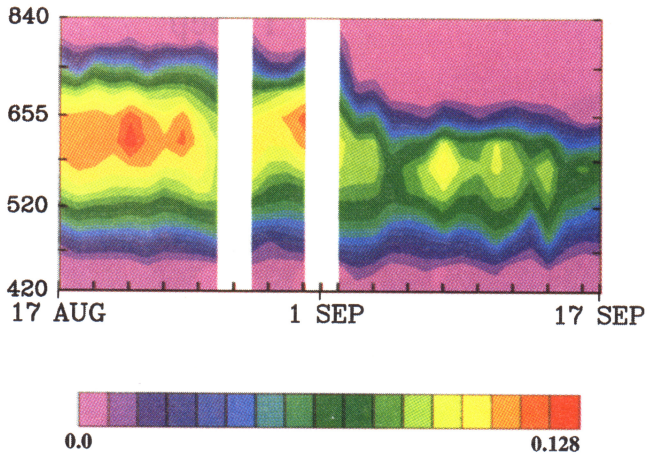

Plate 5. As in Plate 2 (with a different color scale) for $ClONO_2$ mixing ratios in excess of 1.5 ppbv. Data gaps (white spaces in plots) occur during the implementation of instrument modes other than normal science operations.

slope. Trajectory calculations for the 1992 southern hemisphere late winter by *Manney et al.* [1994b] show very little horizontal mixing at 465 K in the vicinity of the intermediate PV contour until the last week in September. Therefore, under the assumption that the trends exhibited by these species arise solely from diabatic descent, the slopes of these lines are used in the tracer continuity equation to estimate average vertical velocities. The vertical velocities estimated from the two tracers are generally consistent and are averaged together to obtain the overall estimate of the vertical velocity at each Θ level. Uncertainties are assigned by propagating into the velocity calculation the uncertainties in the slopes of the lines fit to the daily vortex-averaged mixing ratios and the standard deviations of the tracer vertical profiles, and then augmenting the resulting error if necessary to ensure that the overall average encompasses the estimates from both tracers. This is a deliberately conservative process intended to provide an upper limit on the uncertainty estimate.

Using this approach we find the vortex-averaged descent rate to be 0.5 ± 0.3 mms^{-1} at 585 K and 0.7 ± 0.2 mms^{-1} at 465 K when only the latter half of the yaw period is considered (velocities are higher when trends are taken over the entire yaw period, particularly at 585 K). These are vortex-averaged values; locally, velocities could depart significantly from the vortex averages. While much larger descent rates have been suggested [*Tuck*, 1989], most studies have yielded vertical velocities that are comparable to our values. For example, the velocities calculated here are in agreement, within the uncertainties, with estimates of the lower stratospheric vertical velocity (1.0 mms^{-1}) in August 1992 obtained from simulated air parcel trajectories by *Manney et al.* [1994b]. They also agree very well with the average lower stratospheric descent rates (1.5–1.8 km month^{-1}, or 0.6–0.7 mms^{-1}) estimated for the 1992 winter season from UARS HALOE CH_4 trends [*Schoeberl et al.*, 1995]. However, they are larger than the late-winter residual vertical velocities diagnosed from 1987 NMC temperatures and Airborne Antarctic Ozone Experiment (AAOE) H_2O and O_3 data by *Schoeberl et al.* [1992], which range from 0.1 to 0.2 mms^{-1} between 18 and 22 km at 70°S. More recent radiative transfer calculations by *Rosenfield et al.* [1994], based on NMC temperatures during both the 1987 and the 1992 Antarctic winter seasons, also produce smaller average diabatic descent rates in the lower stratospheric vortex (~0.4–0.9 km month^{-1}, or ~0.2–0.3 mms^{-1}) than those estimated here from the CLAES tracer data. However, the rates deduced by *Rosenfield et al.* [1994] represent an average computed from the descent of air over an 8-month period from March to October, and a direct

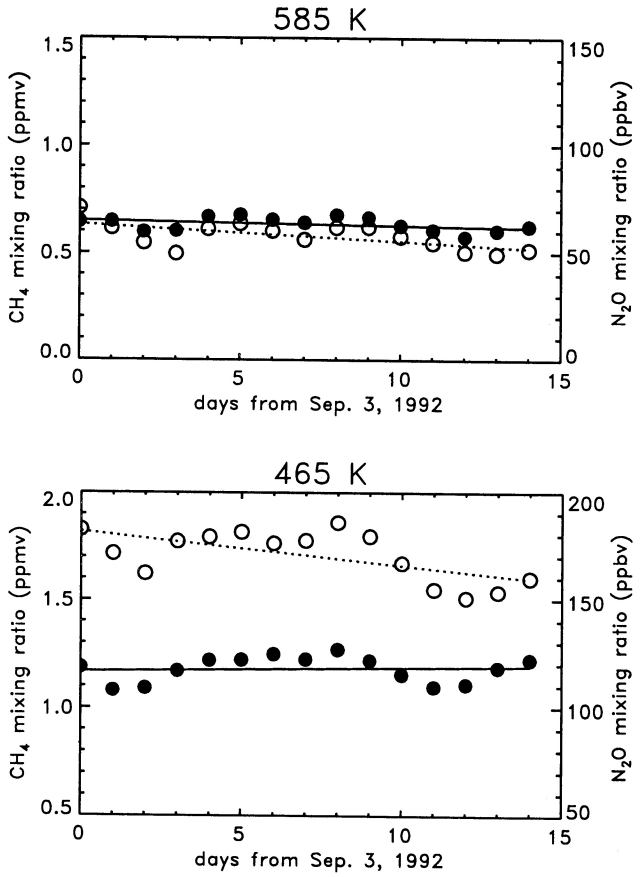

Figure 1. Time series, over the latter half of the 1992 southern hemisphere late-winter south-looking period (starting on September 3), of vortex-averaged (using the intermediate PV contour shown in Plate 1a; see text) mixing ratios of CLAES CH_4 (ppmv) and N_2O (ppbv) at 585 K and 465 K. The vortex-averaged values for each day are represented by circles (filled, CH_4; open, N_2O), and the lines are the least squares fits through the data (solid, CH_4; dotted, N_2O). The slopes of the lines, in combination with the vertical profiles of CH_4 and N_2O, lead to estimates of the diabatic vertical velocity of 0.5 ± 0.3 mms^{-1} at 585 K and 0.7 ± 0.2 mms^{-1} at 465 K.

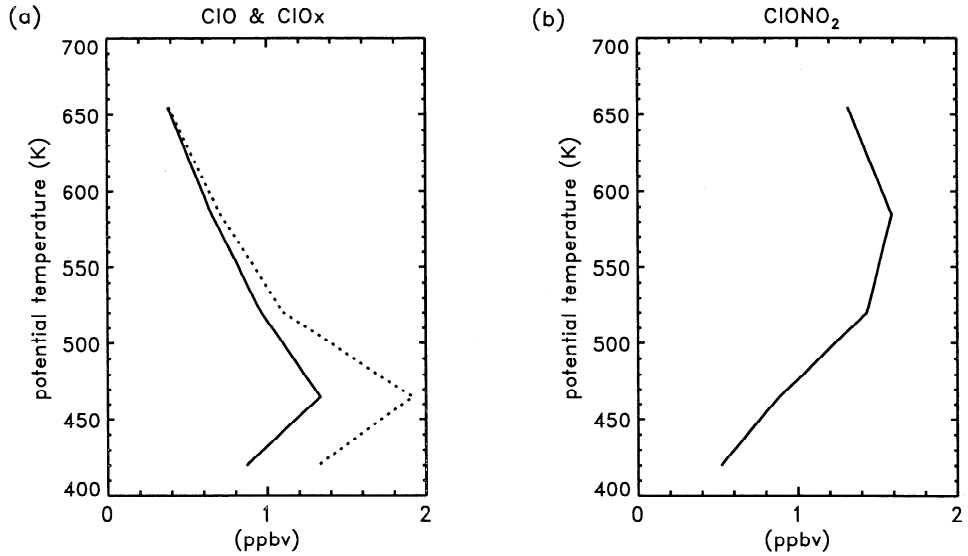

Figure 2. Vertical profiles of (a) MLS ClO (solid line) and inferred ClO_x (dotted line) and (b) CLAES $ClONO_2$ as a function of potential temperature. The profiles were obtained by averaging individual retrievals both spatially (within the area enclosed by the intermediate PV contour of Plate 1a) and temporally (over September 3–17).

comparison with our late-winter velocity estimates is an oversimplification.

When the descent rate at each level has been estimated, the changes in ClO_x and $ClONO_2$ due to vertical transport can also be calculated from the tracer continuity equation, assuming constant velocities throughout the 2-week interval. This calculation would not be necessary for species that are short-lived compared to a 2-week interval, because local photochemical conditions, not dynamics, drive changes in their abundances. As discussed further below, the approximate nature of the approach used here to account for the effects of dynamics is not a major factor in the overall conclusions. The impact of diabatic descent on the mixing ratios of a constituent depends not only on the magnitude of the vertical velocity but also on the shape of the constituent's vertical profile. The averaged ClO and inferred ClO_x mixing ratio profiles (Figure 2a) drop sharply above 465 K, and the downward transport of air with lower ClO abundances accounts for a portion of the observed decline in ClO values at both 585 K and 465 K. Because the peak of the averaged $ClONO_2$ profile (Figure 2b) occurs near 585 K, descent is estimated to produce a decrease in $ClONO_2$ concentrations at that level but an increase in $ClONO_2$ concentrations at 465 K.

Plate 6 shows daily vortex averages of the MLS ClO and inferred ClO_x and CLAES $ClONO_2$ abundances, along with adjusted values obtained by subtracting the estimated changes in mixing ratio due to diabatic descent. These adjusted mixing ratio values reflect the trends in the species that can be attributed to chemical processes. The results presented in Plate 6 are based on averages within the intermediate PV contour in Plate 1a, restricted to the latter half of the yaw period (after September 3). Similar behavior is found for vortex averages within the other two PV contours. For this period the implied chemical loss in ClO alone is approximately 0.3 ± 0.1 ppbv at 585 K and 0.2 ± 0.1 ppbv at 465 K, based on linear fits to the daily averages. Similarly, the implied chemical loss in ClO_x is approximately 0.4 ± 0.1 ppbv at 585 K and 0.4 ± 0.2 ppbv at 465 K. These results indicate a more rapid decay in ClO_x than in ClO, particularly at 465 K. That is, as the ClO_x diminishes throughout the study period, the partitioning between ClO and Cl_2O_2 increasingly favors ClO and the apparent decrease in ClO is reduced.

Although there is a clear decreasing trend in reactive chlorine throughout this interval at both levels, there is an apparent decrease of 0.1 ± 0.1 ppbv in the adjusted $ClONO_2$ mixing ratios at 585 K, and there is no significant chemical change in $ClONO_2$ at 465 K ($\sim 0.0 \pm 0.1$ ppbv). No increase in $ClONO_2$ is found to offset the decrease in ClO_x even when the values at the limits of the uncertainties are used. These adjusted ClO_x and $ClONO_2$ concentrations are computed using the nominal magnitudes of the vertical velocities; however, calculations over the range of velocity values defined by the uncertainties yield very similar results. For completeness we note that, although there is a small increase (~ 0.2 ppbv) in the uncorrected observed $ClONO_2$ mixing ratios (Plate 6) at 465 K (which we attribute to transport effects as discussed above), the decrease in the uncorrected inferred ClO_x values is still larger (~ 0.5 ppbv). In fact, sensitivity tests indicate that for there to be an increase in $ClONO_2$ balancing the decrease in ClO_x, there would have to be strong descent (~ 2.2 mms^{-1}) at 585 K but very strong ascent (~ 7.2 mms^{-1}) at 465 K.

To ensure that a consistent set of air parcels is being

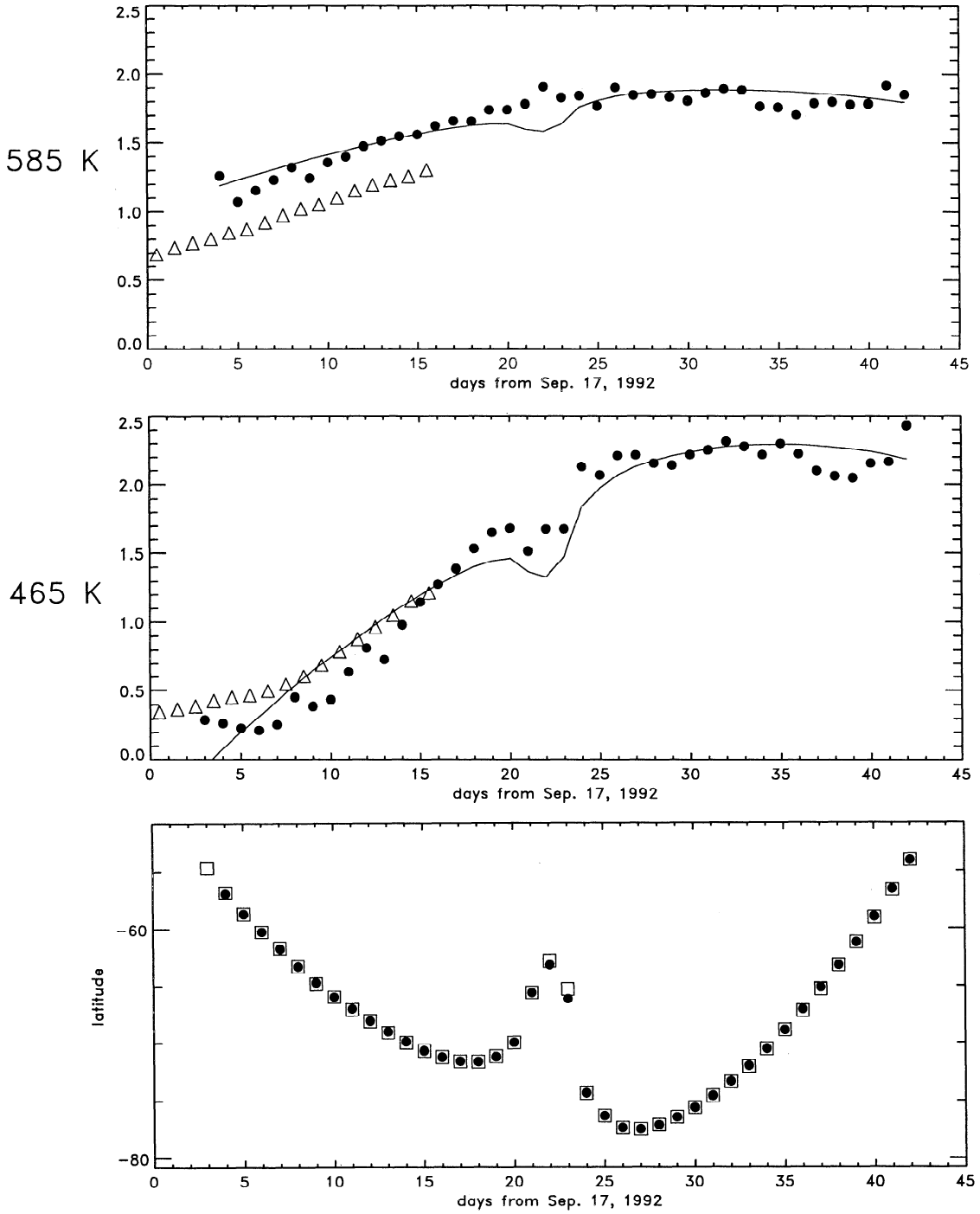

Figure 3. Time series, over the Halogen Occultation Experiment (HALOE) 1992 southern vortex sampling period, of vortex-averaged (within the intermediate PV contour) mixing ratios of HALOE HCl (ppbv; solid circles) at 585 K (top) and 465 K (middle). Also shown (bottom) are the associated daily average latitudes of the profiles (open squares, 465 K; solid circles, 585 K). HALOE data are strong functions of both latitude and time, and multiple linear regression is used to fit curves (solid lines) to the daily averages at both levels. The open triangles shown at both 585 K and 465 K represent calculated HCl values from the SLIMCAT model [*Chipperfield et al.*, this issue], which was run out through the beginning of October.

evaluated for all species, in the preceding calculations all vortex averages include data from the "day" side of the orbit only. However, if any of the chlorine released from ClO_x is being converted into $ClONO_2$, then $ClONO_2$ mixing ratios at night could be slightly larger than those during the day, when $ClONO_2$ is subject to photodissociation. We therefore examine vortex averages of $ClONO_2$ mixing ratios from the "night" side of the orbit, adjusted using the diabatic vertical velocities calculated above. Although the $ClONO_2$ mixing ratios are larger in this case, there is still an apparent decrease of 0.1 ± 0.2 ppbv at 585 K and a decrease of 0.6 ± 0.1 ppbv

at 465 K. As before, no increase in $ClONO_2$ is found to offset the decrease in ClO_x even when the values at the limits of the uncertainties are used.

3.4. Chemical Transport Model Results

We use the SLIMCAT isentropic-coordinate three-dimensional chemical transport model [*Chipperfield et al.*, this issue] to investigate the decay of enhanced ClO in the Antarctic vortex. ECMWF meteorological analyses are used to specify the horizontal winds and temperatures with a spectral truncation of T42, yielding a model horizontal resolution of about 2.8° × 2.8°. The model employs a detailed stratospheric chemistry scheme with treatment of heterogeneous reactions on PSCs and sulfate aerosols. It is initialized with UARS data for August 31, 1992, interpolated onto the T42 Gaussian grid and is run on both the 585 K and the 465 K surfaces. *Chipperfield et al.* [this issue] report results from the basic model as well as those from several sensitivity tests; here we present results only from their run D. This run treats 465 K and 585 K as separate unconnected isentropic surfaces with no vertical transport between them. It also includes the reaction $OH+ClO \rightarrow HCl+O_2$ as an 8% channel. Although only speculative at this time, this pathway has been shown to improve the agreement between photochemical models and observations of ClO, HCl, and O_3 in the upper stratosphere [*McElroy and Salawitch*, 1989; *Natarajan and Callis*, 1991; *Chandra et al.*, 1993; *Toumi and Bekki*, 1993; *Minschwaner et al.*, 1993; *Eckman et al.*, 1995]. *Chipperfield et al.* [this issue] show that the inclusion of this channel is also important in the lower stratosphere, affecting model results at both 585 K and 465 K.

Vortex averages of model chlorine species from this run are shown in Plate 7, along with MLS ClO and inferred ClO_x and CLAES $ClONO_2$. The model fields have been sampled at the same local time as the MLS and CLAES measurements. Total inorganic chlorine Cl_y ($Cl_y = HCl + ClONO_2 + ClO + 2Cl_2O_2 + OClO + BrCl + Cl + HOCl$) is essentially constant at 3.2 ppbv at 585 K and 3.0 ppbv at 465 K. The model reproduces the vortex-averaged MLS ClO abundances and downward trend at 585 K, but at 465 K it underestimates MLS ClO by as much as 0.4 ppbv (see *Chipperfield et al.* [this issue] for an elaboration of the low model ClO). At 465 K the model also indicates an increasing trend in ClO (not seen in the data) that arises because the model overestimates the extent of the ongoing PSC processing. Model ClO_x values are in good agreement with those inferred from MLS ClO, even at 465 K (where the model partitions a considerable fraction of ClO_x into Cl_2O_2). Similarly, the model reproduces the CLAES $ClONO_2$ data fairly well at 585 K, although it indicates a small increase in $ClONO_2$ over the interval that is not seen in the data. However, at 465 K, while the model also indicates little or no trend, it underestimates CLAES $ClONO_2$ by as much as 0.6 ppbv. This discrepancy in $ClONO_2$ values also arises from overestimating the degree of activation; in the model, heterogeneous processing has removed nearly all of the $ClONO_2$ in the inner vortex, whereas CLAES data indicate mixing ratios between 0.25 and 1.0 ppbv in the inner vortex. As discussed by *Chipperfield et al.* [this issue], inclusion of the $OH + ClO \rightarrow HCl + O_2$ reaction suppresses the increase in $ClONO_2$ and promotes the conversion of ClO to HCl. The calculated changes in $ClONO_2$ and HOCl are not significant, and the main recovery is predicted to be into HCl at both 585 K and 465 K.

3.5. Behavior of HCl

The model results of *Chipperfield et al.* [this issue] suggest that $ClONO_2$ is not the dominant chlorine reservoir during the first few weeks of recovery. *Santee et al.* [1995] report that in mid-August 1992, gas-phase HNO_3 values measured by MLS were extremely low ($\leq$ 2 ppbv) throughout a low-temperature ($\leq$ 195 K) region encompassing most of the Antarctic vortex. The deficit in gas-phase HNO_3 persisted into November, well after lower stratospheric temperatures had risen above the PSC evaporation threshold, implying that denitrification had occurred in the polar vortex. Removal of gas-phase HNO_3 prevents NO_2 release from HNO_3 photolysis and, consequently, inhibits formation of $ClONO_2$. Detailed model simulations [*Prather and Jaffe*, 1990] of perturbed air parcels spun out from the vortex and transported to lower latitudes have shown that when denitrification occurs, $ClONO_2$ is a less significant chlorine reservoir during the first 20 days, and recovery is limited by formation of HCl. Therefore we consider the possibility that the reactive chlorine is being converted into HCl rather than $ClONO_2$, as seen by *Douglass et al.* [1995].

HALOE observations of HCl within the southern polar vortex become available on about September 20, a few days after the emission instruments turn away from the south and resume viewing northern high latitudes. HALOE sampling of the southern polar region ceases around October 30. Individual sunrise or sunset profiles are interpolated to Θ surfaces, and a simple average of all of the profiles falling within the intermediate PV contour shown in Plate 1a is calculated. The number of points constituting such a "vortex average" varies with the latitude of the profiles; the maximum number is 15. The standard deviation in the mean also varies from day to day, with a maximum of 0.2 ppbv and 0.5 ppbv at 585 K and 465 K, respectively. The daily vortex-averaged mixing ratios at 585 K and 465 K, along with their associated daily average latitudes, are presented in Figure 3 for the entire period of southern vortex coverage. Vortex-averaged HCl abundances are seen to increase during this period, particularly at 465 K. Vortex averages of model HCl (which is calculated out through the beginning of October [*Chipperfield et al.*, this issue]) agree well with those of HALOE HCl at 465 K but underestimate those of HALOE HCl at 585 K by 0.2–0.3 ppbv.

Because the HALOE data are strong functions of latitude as well as time, multiple linear regression (with both latitude and time functions included) is used to fit

a curve to the daily averages as in the work of *Schoeberl et al.* [1995]. We initially use the $\partial(HCl)/\partial t$ value obtained from this fit to extrapolate the HCl values back to the time frame of the MLS and CLAES data. However, at 465 K the change in HCl with time is sufficiently rapid that the extrapolation produces negative mixing ratios. In contrast, at 585 K the change in HCl with time is so gradual that at the beginning of the interval the extrapolation produces mixing ratios of almost 1 ppbv, a value that may be unrealistically high since a substantial fraction of HCl is expected to have been removed by PSC processing at this time. Following the results of *Liu et al.* [1992] and those from the SLIMCAT model (Plate 7), which show HCl increasing fairly steadily throughout the interval from near zero at both levels, the HCl is extrapolated back from the first HALOE data point inside the vortex (on September 20) by assuming it varies linearly from zero at the start of the study period on September 3.

In Plate 8 we show the vortex-averaged HCl mixing ratios during the HALOE southern vortex sampling period and linearly extrapolated HCl values during the late-winter study period. Also included in Plate 8 are the mixing ratios of inferred ClO_x and $ClONO_2$ (adjusted for the effects of vertical transport as described above), the sum ClO_x + $ClONO_2$, and the sum ClO_x + $ClONO_2$ + extrapolated HCl. At both 585 K and 465 K the sum ClO_x + $ClONO_2$ exhibits a decreasing trend over the course of the interval. If $ClONO_2$ and HCl are the primary reservoirs for chlorine at this time, then ClO_x + $ClONO_2$ + HCl should be roughly a conserved quantity. At 585 K, inclusion of HCl extrapolated from zero on September 3 leads to an apparent increase in the chlorine budget of almost 0.6 ppbv over the interval (based on linear fits to the daily values), with a final value of ~3.1 ppbv. However, the trend in ClO_x + $ClONO_2$ + HCl at this level is highly sensitive to the initial value chosen for the HCl extrapolation. Assuming HCl ~ 1 ppbv on September 3 (the result obtained from the $\partial(HCl)/\partial t$ extrapolation) leads to a value of ClO_x + $ClONO_2$ + HCl that decreases over the course of the interval but has a magnitude of roughly 3.5 ppbv (slightly above the estimated total chlorine loading at that level [*Gunson et al.*, 1994]). Assuming HCl=0.6 ppbv on September 3, a value significantly higher than the model prediction of Plate 7, leads to a fairly constant value of 3.2 ppbv for ClO_x + $ClONO_2$ + HCl. Thus the chlorine budget can be made to balance at 585 K, given the uncertainties and assuming a range of acceptable values for HCl.

At 465 K, although the addition of HCl extrapolated back to zero on September 3 does result in a marginal improvement in the chlorine balance, the contribution from HCl is not sufficient to offset the observed losses. The quantity ClO_x + $ClONO_2$ + extrapolated HCl declines slightly over the 2-week study period (although the uncertainties in these quantities are such that a line with zero slope could be fit to these data points). The HALOE data actually exhibit a slight decreasing trend from 0.3 ppbv for the first few days of southern vortex sampling, and we investigate a constant value of 0.3 ppbv during the study period as an alternative to the backward extrapolation to zero. In this case the lack of closure in the chlorine budget is exacerbated. This example illustrates that the imbalance between the decrease in reactive chlorine and the increase in the chlorine reservoirs at 465 K cannot be ameliorated simply by adjusting the extrapolation of the HCl data.

3.6. Discussion

The lack of balance between the decrease in ClO_x and the increase in $ClONO_2$ in the Antarctic vortex may not be unexpected. *Santee et al.* [1995] find evidence for severe denitrification in the 1992 Antarctic vortex. Under highly denitrified conditions, the major source of NO_2 is removed and the reformation of $ClONO_2$ is suppressed. However, if $ClONO_2$ is not playing a primary role, then either the free chlorine is being converted into another reservoir or it is being resupplied. *Prather and Jaffe* [1990] show that under conditions of substantial ozone loss the chemical system is highly nonlinear and the Cl-ClO-$ClONO_2$ partitioning favors Cl, leading to the preferential formation of HCl. *Douglass et al.* [1995] have also recently studied the springtime production of chlorine reservoir species. They use UARS data to constrain a chemical box model and compare both observations and model results within a narrow annulus just inside the southern vortex boundary (the "collar" region) for a 3-month period during the 1992 Antarctic winter to those from a similar region and timespan during the 1991 1992 Arctic winter. Results from model runs at 460 K indicate that, in the absence of denitrification, ozone concentrations dictate which chlorine reservoir dominates in spring. When O_3 mixing ratios remain above about 0.5 ppmv, $ClONO_2$ production arising from HNO_3 photolysis occurs rapidly. However, following the arguments of *Prather and Jaffe* [1990], *Douglass et al.* [1995] find that O_3 mixing ratios below 0.5 ppmv promote the production of HCl.

The conclusions of *Douglass et al.* [1995] pertain strictly to conditions of mild denitrification (as in the Arctic or the Antarctic collar region) and extremely low ozone (as in the Antarctic in October), and consequently they cannot be applied to the early-to-mid-September time period studied here. While a significant reduction in ozone is occurring throughout September 1992, on the last day of our study period (September 17), O_3 concentrations are still above 0.5 ppmv in most of the area of the vortex [*Waters et al.*, 1993b], and the vortex-averaged O_3 mixing ratio at 465 K [*Manney et al.*, 1993] is still above 1.5 ppmv. However, the formation of HCl may still be the dominant mechanism for chlorine recovery at this time. Results from the SLIMCAT isentropic chemical transport model [*Lary et al.*, 1995; *Chipperfield et al.*, this issue] show that production of $ClONO_2$ is suppressed and ClO is converted into HCl when the reaction OH + ClO → HCl + O_2 is included as an 8% channel. Nevertheless, the data seem to indicate that the observed decay in enhanced ClO is

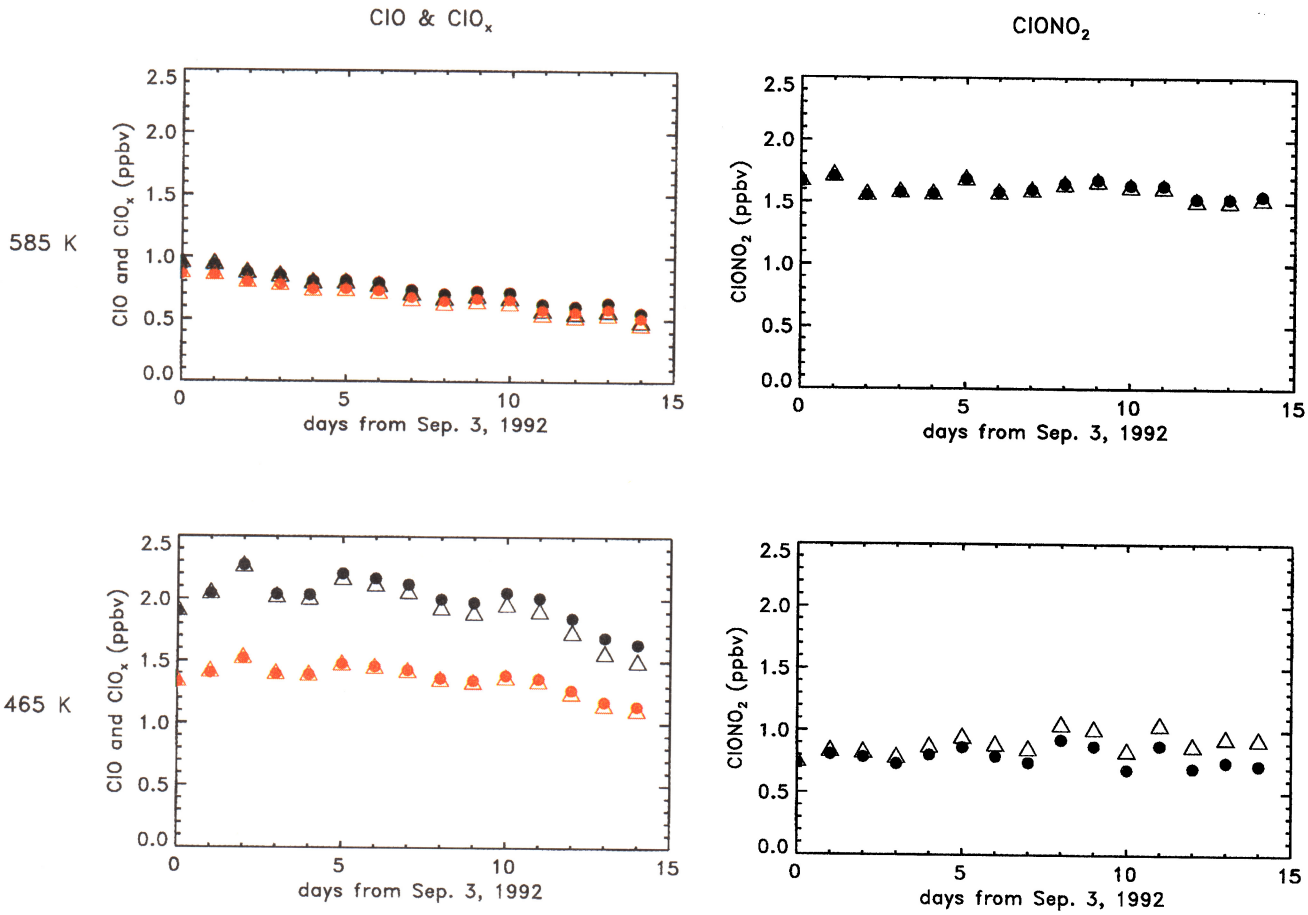

Plate 6. Time series, over the latter half of the 1992 southern hemisphere late-winter south-looking period (starting on September 3), of vortex-averaged (using the intermediate PV contour shown in Plate 1a) mixing ratios (ppbv) of MLS ClO (red) and inferred ClO_x (black) and CLAES $ClONO_2$ at 585 K and 465 K. The vortex-averaged values observed on each day are represented by open triangles, and the mixing ratios adjusted for the effects of diabatic descent are represented by solid circles.

not entirely offset by a corresponding increase in HCl at 465 K.

There are several factors that may account for the apparent lack of balance between the decay of reactive chlorine and the production of chlorine reservoirs at 465 K in the Antarctic vortex. As discussed in connection with Plate 3, intermittent localized PSC events occur at the 465 K level through the end of the study period. Because of the spacing of the UARS orbit tracks, additional short-lived PSCs with limited geographical extent may have gone undetected. The episodic nature of the PSC activity at the end of southern winter may have created a complicated pattern of recurring chlorine activation and deactivation. In fact, vortex-averaged 465 K ClO abundances, while following a general downward trend, are observed to oscillate by a tenth of a part per billion or so on timescales of a few days. The true behavior of the chlorine species may be obscured by either the limited horizontal resolution of the data sets or the fact that we are examining vortex-averaged quantities at a time when processes are occurring on more localized scales.

Alternatively, the answer may lie in incomplete model chemistry or previously unidentified reservoirs of either active or inactive chlorine. *Toon et al.* [1992] estimate the total amount of inorganic chlorine from the HF burden measured using an airborne Fourier transform infrared (FTIR) spectrometer during AASE II. They then deduct from this value their measured HCl, $ClONO_2$, and HOCl burdens to calculate the amount of "missing" chlorine. Comparing this quantity to an estimated ClO column amount derived from the maximum mixing ratio observed during AASE II plus an equal amount of the ClO dimer, they find that the amount of "missing" chlorine indicated by the FTIR measurements exceeds that likely to reside in ClO and Cl_2O_2. Although this result is obtained for the Arctic vortex, a similar deficit of inorganic chlorine over Antarctica in 1987 is noted by *Toon et al.* [1989]. *Toon et al.* [1992] conclude that other unmeasured forms of inor-

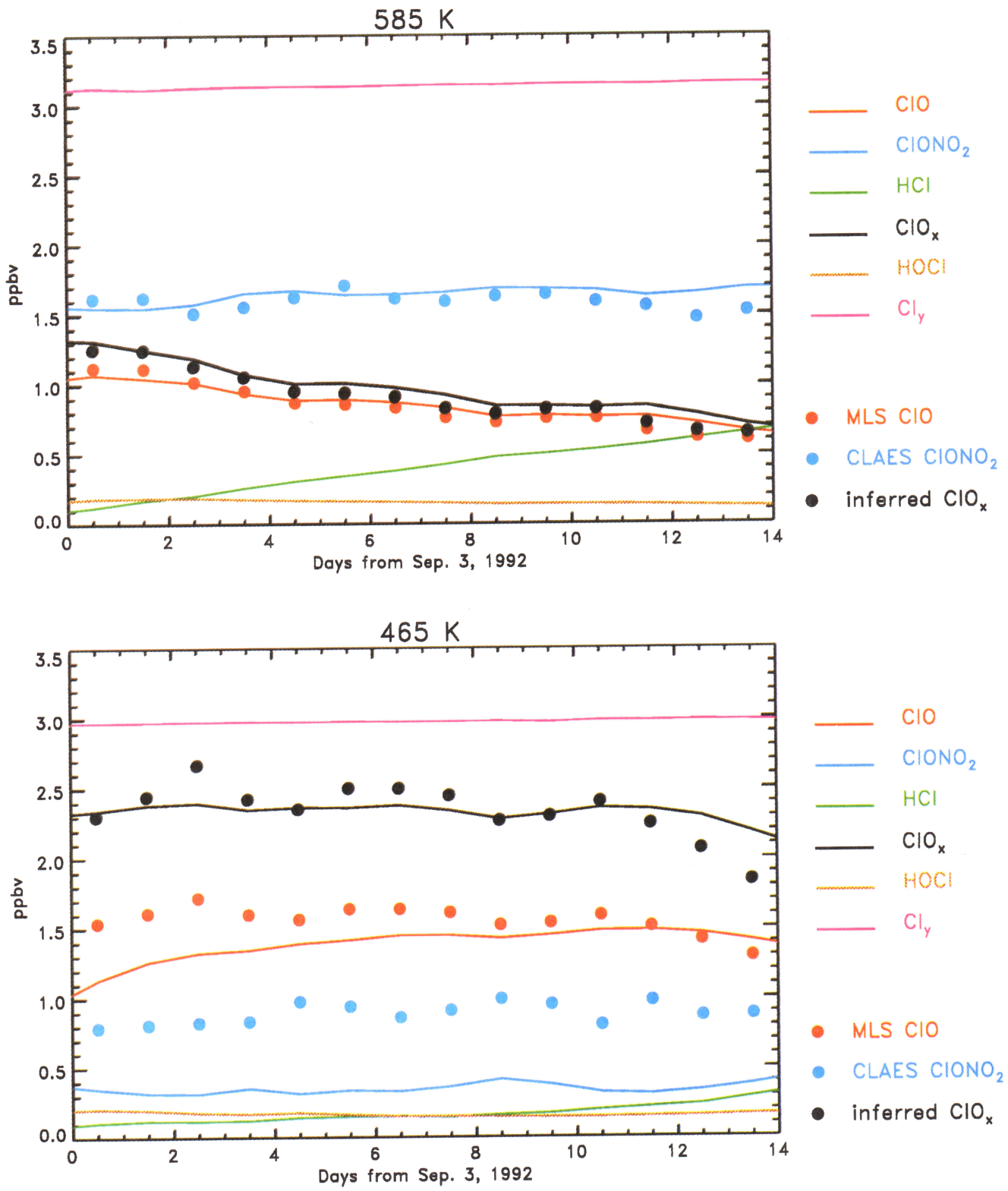

Plate 7. Vortex-averaged chlorine species at 585 K (top) and 465 K (bottom) from the SLIMCAT chemical transport model [*Chipperfield et al.*, this issue]. Model species are sampled at the same local time as the MLS and CLAES measurements. Also shown are the vortex-averaged MLS ClO and inferred ClO_x and CLAES $ClONO_2$ values. These differ slightly from the vortex averages shown in Plate 6 because they are calculated from the ClO and $ClONO_2$ fields interpolated onto the model T42 Gaussian grid and because of differences in the PV contours defined from the NMC analyses (used here) and the ECMWF analyses (used by *Chipperfield et al.* [this issue]).

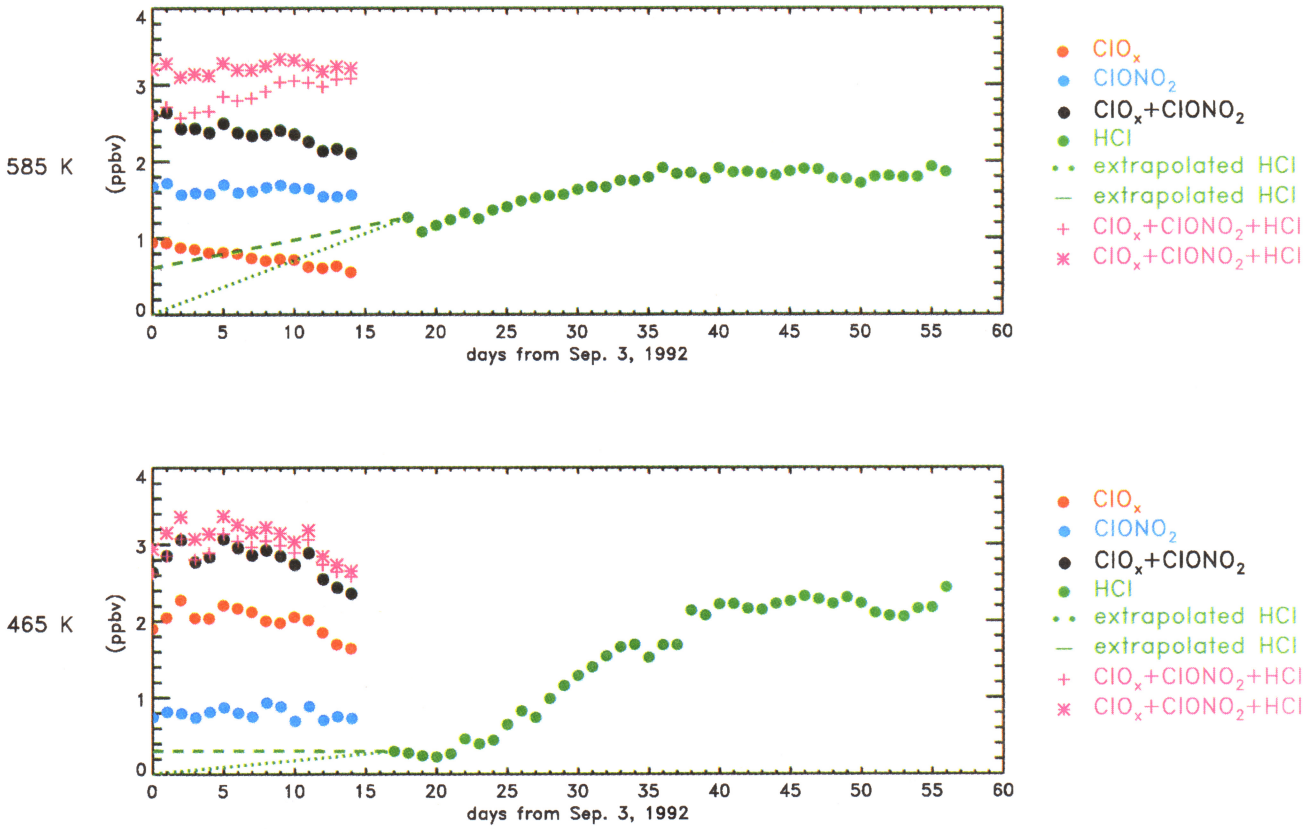

Plate 8. Vortex-averaged HCl mixing ratios during the HALOE 1992 southern vortex sampling period (green circles) at 585 K (top) and 465 K (bottom). Also shown are the HCl linearly extrapolated back to zero on September 3 (dotted green lines); the HCl linearly extrapolated back to 0.6 ppbv (585 K)/0.3 ppbv (465 K) (dashed green lines); the adjusted vortex-averaged mixing ratios of MLS ClO_x (red circles) and CLAES $ClONO_2$ (cyan circles); the sum ClO_x + $ClONO_2$ (black circles); and the quantity ClO_x + $ClONO_2$ + extrapolated HCl (magenta plus signs correspond to dotted green lines and magenta asterisks correspond to dashed green lines).

ganic chlorine may be present in the winter polar vortex, as suggested by *Sander et al.* [1989].

Finally, the quality of the data themselves may be hampering the effort to close the chlorine budget. Difficulties in initializing the chemical transport model [*Chipperfield et al.*, this issue] reveal that the UARS data set is not entirely self-consistent. For example, the total inorganic chlorine derived from CLAES N_2O measurements using empirical relationships [*Webster et al.*, 1993; *Woodbridge et al.*, 1995] significantly underestimates the sum of MLS ClO and CLAES $ClONO_2$ at 465 K. The precision of both the MLS and the CLAES data sets is a limiting factor in the analysis of mixing ratio trends, and it affects our ability to make unequivocal statements about the chlorine budget.

To explore this issue fully requires data extending further into the recovery period. In 1992 the viewing geometry precluded MLS and CLAES from making Antarctic measurements during the interval from the middle of September to the end of October. By the time south viewing resumed, ClO was no longer enhanced. Unfortunately, this is the only southern winter for which simultaneous CLAES and MLS data exist; the CLAES supply of cryogen was depleted in May 1993, and there are no CLAES measurements after that time. However, we can use UARS data to investigate the behavior of ClO and the chlorine reservoirs in the northern hemisphere.

4. 1992–1993 Northern Hemisphere Winter

4.1. Behavior of ClO and $ClONO_2$

MLS observed lower stratospheric ClO enhanced to greater than 1 ppbv as early as December 4, 1992 [*Waters et al.*, 1993a, 1995], when temperatures briefly fell below the approximate threshold for PSC existence. Temperatures fluctuated around the PSC threshold until late December, after which they were almost continuously below the threshold until late February 1993. When MLS resumed north-viewing measurements in mid-February, lower stratospheric ClO abundances greater than 1 ppbv were seen in most of the vortex region [*Waters et al.*, 1995]. We will examine this late-winter yaw period (February 12 – March 16, 1993) for chlorine balance. As in the southern hemisphere, we use CLAES measurements of aerosol extinc-

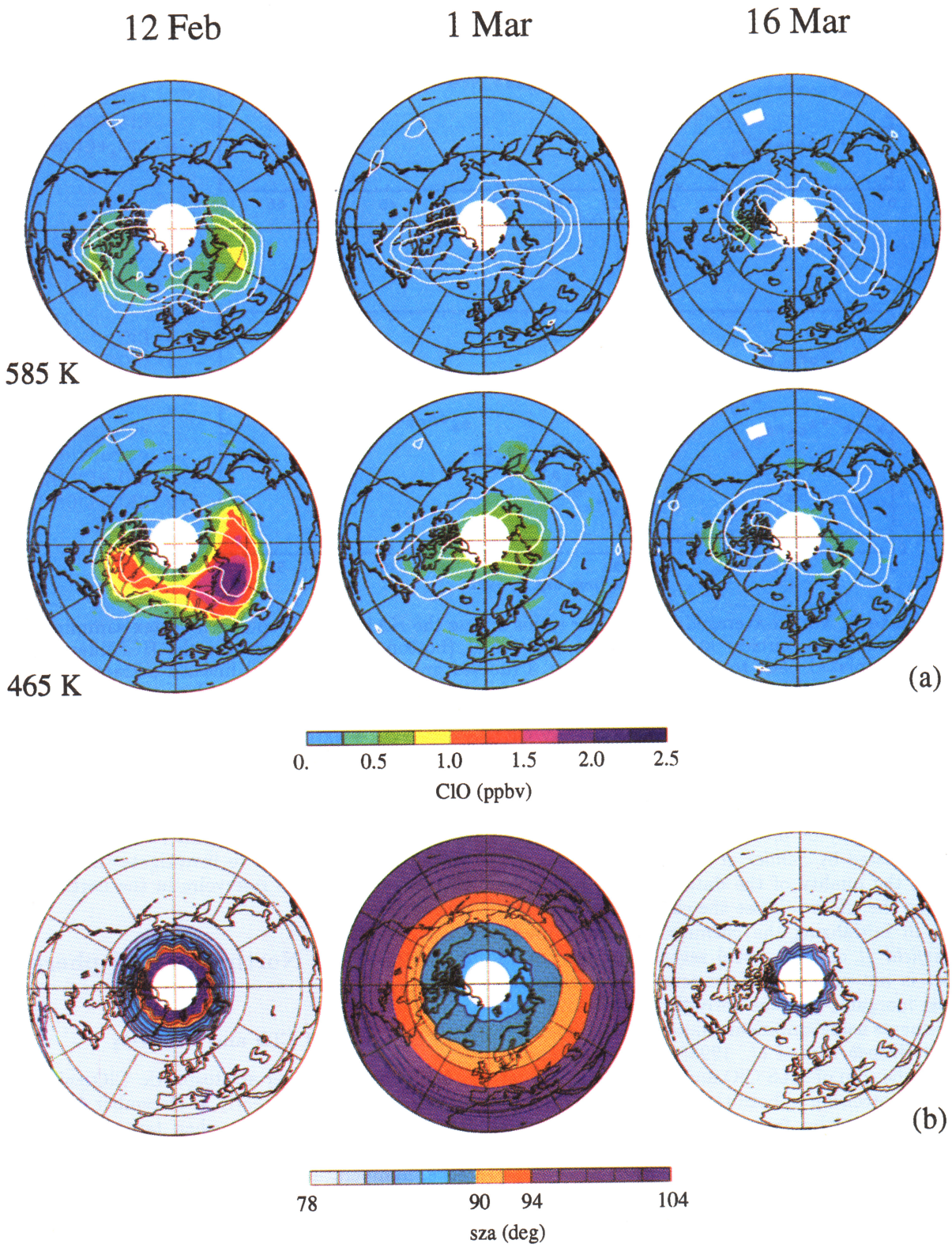

Plate 9. (a) As in Plate 1a for the 1992–1993 northern hemisphere late-winter north-looking period, with the Greenwich meridian at the bottom, and positive PV contour values. (b) As in Plate 1b for the days shown in Plate 9a.

tion (not shown) to look for evidence of continued heterogeneous chlorine activation. Except for a few transient (1–2 days in duration) and highly localized (near Iceland) events during the third week in February, no significant PSC activity is observed during the northern hemisphere late-winter yaw period, and ClO declines throughout this interval.

Maps of MLS ClO for three selected days at the beginning, middle, and end of the northern hemisphere late-winter observing period are shown in Plate 9a. Again, only data from the "day" side of the orbit are included in these maps. The northern hemisphere study period is nearly identical to that of the southern hemisphere in terms of season (days since winter solstice); the measurement solar zenith angles are comparable for each set of selected days (compare Plates 9b and 1b). The same three contours of PV shown in Plate 1a are also superimposed on these maps, but in the northern hemisphere the innermost PV contour shrinks considerably over time and is not suitable for vortex averaging. The PV contours indicate that the vortex is highly distorted and displaced from the pole throughout this period. Although there are patches in which ClO abundances reach Antarctic levels, ClO is not so uniformly enhanced within the vortex as is observed in the southern hemisphere. In addition, ClO appears to diminish more rapidly at both levels in the northern hemisphere than in the southern hemisphere. At 585 K, chlorine is almost completely deactivated by March 1. These trends are also evident in Plate 10. Maps of CLAES $ClONO_2$ during the late-winter interval are shown in Plate 11. $ClONO_2$ abundances in the Arctic vortex are generally smaller than those in the Antarctic collar region, but there is no pronounced deficit in the vortex interior as there is in the Antarctic (compare Plate 4). $ClONO_2$ mixing ratios and the area in the region poleward of 52°N with $ClONO_2$ concentrations in excess of 1.5 ppbv (Plate 12) show little (or a slightly decreasing) trend at 585 K; however, in contrast to the south, they increase at 465 K.

4.2. Effects of Vertical Transport

Diabatic descent is also expected over the northern polar regions [*Schoeberl and Hartmann*, 1991]. Again, we estimate the vertical velocities at 585 K and 465 K from CLAES measurements of N_2O and CH_4. Daily vortex-averaged (for the intermediate PV contour shown in Plate 9a) mixing ratios for both tracers are plotted in Figure 4. In the north the vertical velocities estimated from the two tracers are not consistent at 585 K, with CH_4 indicating descent but N_2O indicating ascent. The cause of this inconsistency may be that the changes in the daily vortex averages cannot be ascribed solely to vertical motions (an underlying assumption in our calculation of the vertical velocities) since two strong stratospheric warmings during the late-winter observing period lead to increased horizontal mixing [*Manney et al.*, 1994b]. S. E. Strahan et al. (Long-lived tracer transport in the Antarctic stratosphere, submitted to *Journal of Geophysical Research*, 1995) analyzed model simulations and CLAES data and found that when poleward horizontal transport becomes significant (e.g., during periods of strong wave activity), the different meridional (and vertical) gradients in N_2O and CH_4 can result in time tendencies with opposite signs. In this case, the vertical velocities inferred from the two tracers would also disagree in sign. Based on previous studies [e.g., *Schoeberl et al.*, 1992], we assume that descent is occurring at this season, and we neglect the N_2O values in estimating the magnitude of the vertical velocity at 585 K. We find the vortex-averaged descent rate to be 0.1 ± 0.2 mms^{-1} at 585 K and 0.1 ± 0.1 mms^{-1} at 465 K when the trends over the entire yaw period are considered. These values are substantially smaller than the descent rates suggested by *Tuck et al.* [1992]. They are also smaller than estimates of the lower stratospheric vertical velocity (0.6–0.7 mms^{-1}) in February 1993 obtained from simulated air parcel trajectories by *Manney et al.* [1994b], the late-winter residual vertical velocities (0.6–1.0 mms^{-1} between 18 and 22 km at 70°N) diagnosed from AASE data by *Schoeberl et al.* [1992], and the average diabatic descent rates in the lower stratospheric vortex (~1.3–2.0 km month^{-1}, or ~0.5–0.6 mms^{-1}) computed from NMC temperatures over a 5-month period from November to March by *Rosenfield et al.* [1994]. Contrary to the calculations of *Rosenfield et al.* [1994], our results (and those of *Manney et al.* [1994b]) indicate that lower stratospheric vertical velocities are smaller in the northern hemisphere than in the southern hemisphere (at least for the late-winter time periods considered here).

As in the southern hemisphere, the total reactive chlorine is calculated from the daily averaged ClO mixing ratios at each level. The estimated changes in MLS ClO and inferred ClO_x and CLAES $ClONO_2$ due to vertical transport effects are illustrated in Plate 13. The slight dip in the vortex-averaged ClO concentrations just after day 15 of the study period (February 27) appears because measurements obtained in the middle of the yaw cycle have high solar zenith angles. We cannot explain the behavior of the last two $ClONO_2$ data points (March 14, 16); large data gaps exist on surrounding days (March 13, 15), which have been excluded from the vortex averages, but the data coverage on March 14 and 16 is adequate. In general, the inferred Arctic vertical velocities are too weak to have a substantial impact, and the corrections to the observed mixing ratios are small. The implied chemical loss in ClO alone is approximately 0.2 ± 0.1 ppbv at 585 K and 1.1 ± 0.1 ppbv at 465 K, based on linear fits to the daily averages. Similarly, the implied chemical loss in ClO_x is approximately 0.3 ± 0.1 ppbv at 585 K and 1.2 ± 0.1 ppbv at 465 K. As in the southern hemisphere, ClO_x decays more rapidly than ClO, particularly at 465 K. There is a corresponding increase in $ClONO_2$ of 0.2 ± 0.1 ppbv at 585 K and 1.0 ± 0.1 ppbv at 465 K. In contrast to

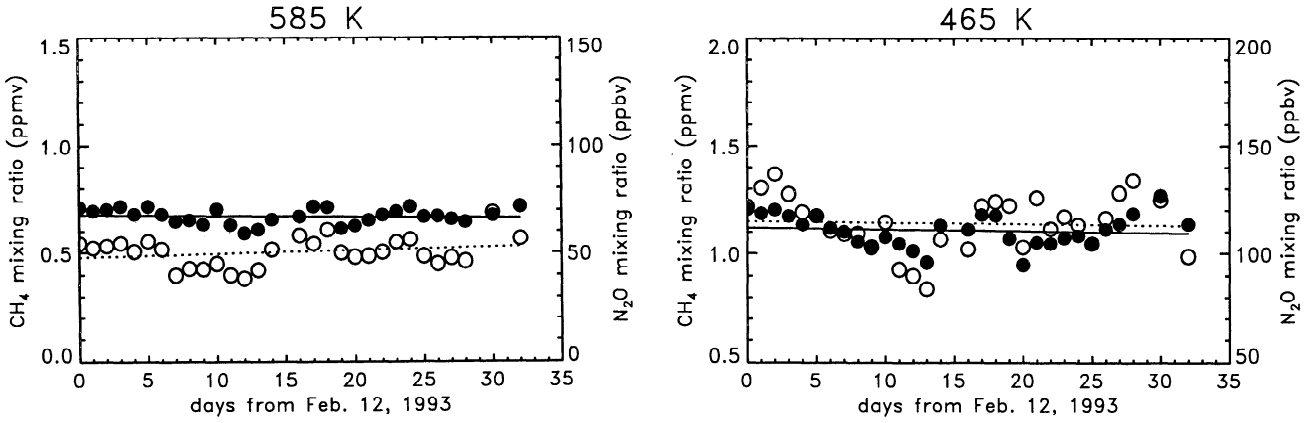

Figure 4. As in Figure 1 for the 1992–1993 northern hemisphere late-winter north-looking period. The slopes of the lines lead to estimates of the diabatic vertical velocity of 0.1 ± 0.2 mms^{-1} at 585 K and 0.1 ± 0.1 mms^{-1} at 465 K.

the southern polar vortex, in the north the calculated chemical changes in ClO_x and $ClONO_2$ are balanced (within the uncertainties) at both levels. The changes in ClO_x and $ClONO_2$ are in even better agreement if the last two $ClONO_2$ data points (see Plate 13) are ignored. These results are not highly sensitive to the values of the descent rates; the implied chemical changes in ClO and $ClONO_2$ are still in balance at both levels, within the limits of the uncertainties, even when vertical velocities as large as those estimated by *Schoeberl et al.* [1992] are used.

4.3. Behavior of HCl

HALOE observations of HCl within the northern polar vortex become available on about March 16, at the end of the MLS and CLAES north-viewing period. HALOE sampling of the northern polar region ceases around April 27. In the northern hemisphere the elongated shape of the vortex limits the number of HALOE measurements obtained within it on any given day. On some days no profiles are recorded inside the intermediate PV contour. Therefore, to avoid large gaps in the time series of averaged mixing ratios, the HCl is averaged within the outermost PV contour shown in Plate 9a. The maximum number of points combined in these "vortex averages" is nine. The daily vortex-averaged mixing ratios at 585 K and 465 K, along with their associated daily average latitudes, are presented in Figure 5 for the entire period of northern vortex coverage. Although HCl exhibits an increasing trend in the weeks after yaw, the increase is much more gradual than that observed in the southern polar region (Figure 3). As in the southern hemisphere, $\partial(\mathrm{HCl})/\partial t$ is calculated through multiple linear regression to account for both the time and the latitude dependence of the HALOE data and used to linearly extrapolate HCl back to the time frame of the MLS and CLAES data. At 585 K, the extrapolation using the $\partial(\mathrm{HCl})/\partial t$ value leads to HCl mixing ratios on February 12 of about 1.1 ppbv, in good agreement with HCl measurements from a balloon flight on February 13, 1992, during EASOE [*Arnold and Spreng*, 1994]. At 465 K, the extrapolation using the $\partial(\mathrm{HCl})/\partial t$ value produces negative HCl mixing ratios at the beginning of the study period (similar to the situation in the southern hemisphere). At this level, HCl mixing ratios between 0.0 and 0.5 ppbv would be consistent with both the balloon observations of *Arnold and Spreng* [1994] and the observations from an ER-2 flight, also on February 13, 1992, during AASE II [*Webster et al.*, 1993]. We explore below the impact of 465 K HCl mixing ratios in this range on the overall chlorine budget. It should be noted that both the EASOE and the AASE II data were obtained during a different winter (1991/1992) than that of the data described here (1992/1993). The effects of Mount Pinatubo and other sources of interannual variability might be expected to lead to very different HCl values for the two years; however, these observations provide at least a reasonable constraint for our extrapolations.

In Plate 14 we show the vortex-averaged (over the outermost PV contour) HCl mixing ratios during the HALOE northern vortex sampling period and linearly extrapolated HCl values during the late-winter study period. Also included in Plate 14 are the vortex-averaged (over the intermediate PV contour) mixing ratios of inferred ClO_x and $ClONO_2$ (adjusted for the effects of vertical transport as described above), the sum ClO_x + $ClONO_2$, and the sum ClO_x + $ClONO_2$ + extrapolated HCl. At 585 K, the sum ClO_x + $ClONO_2$ + HCl is essentially constant, with a value of about 2.9 ppbv. At 465 K, extrapolating HCl back to zero on February 12 leads to a small increase in ClO_x + $ClONO_2$ + HCl (which varies around 2.2 ppbv), whereas extrapolating HCl back to 0.5 ppbv leads to a

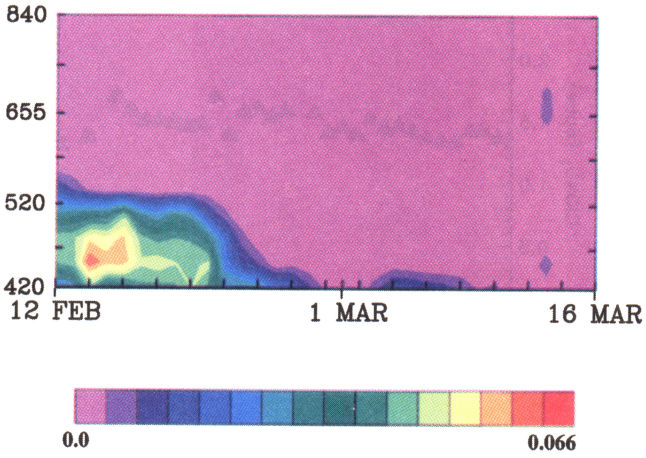

Plate 10. As in Plate 2 (with a different color scale) for the 1992–1993 northern hemisphere late-winter north-looking period.

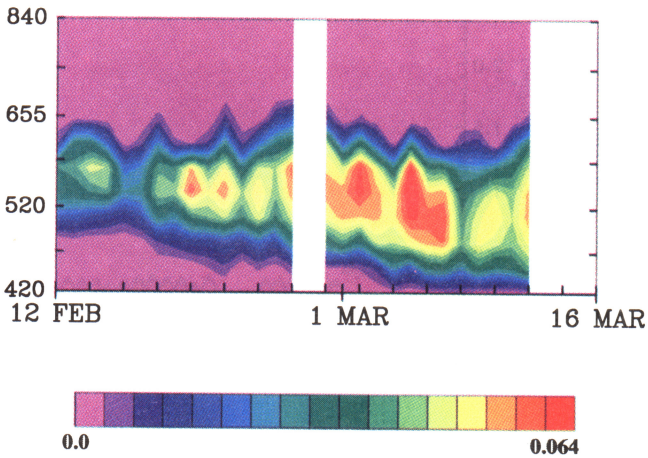

Plate 12. As in Plate 10 for $ClONO_2$ mixing ratios in excess of 1.5 ppbv. Data gaps (white spaces in plots) occur during the implementation of instrument modes other than normal science operations.

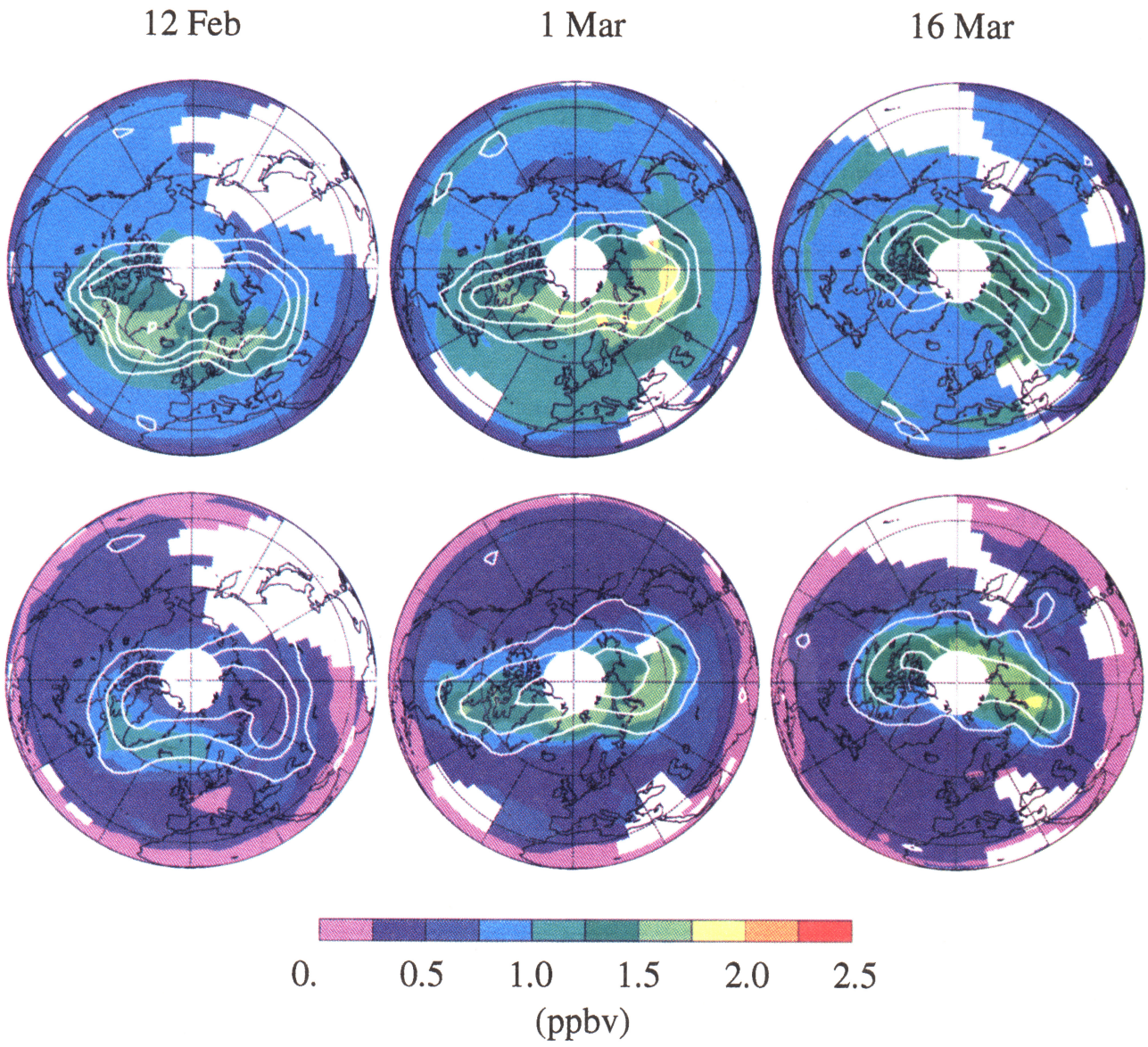

Plate 11. As in Plate 9a for CLAES $ClONO_2$. Blank spaces in the maps represent areas where there are data gaps or spurious data points.

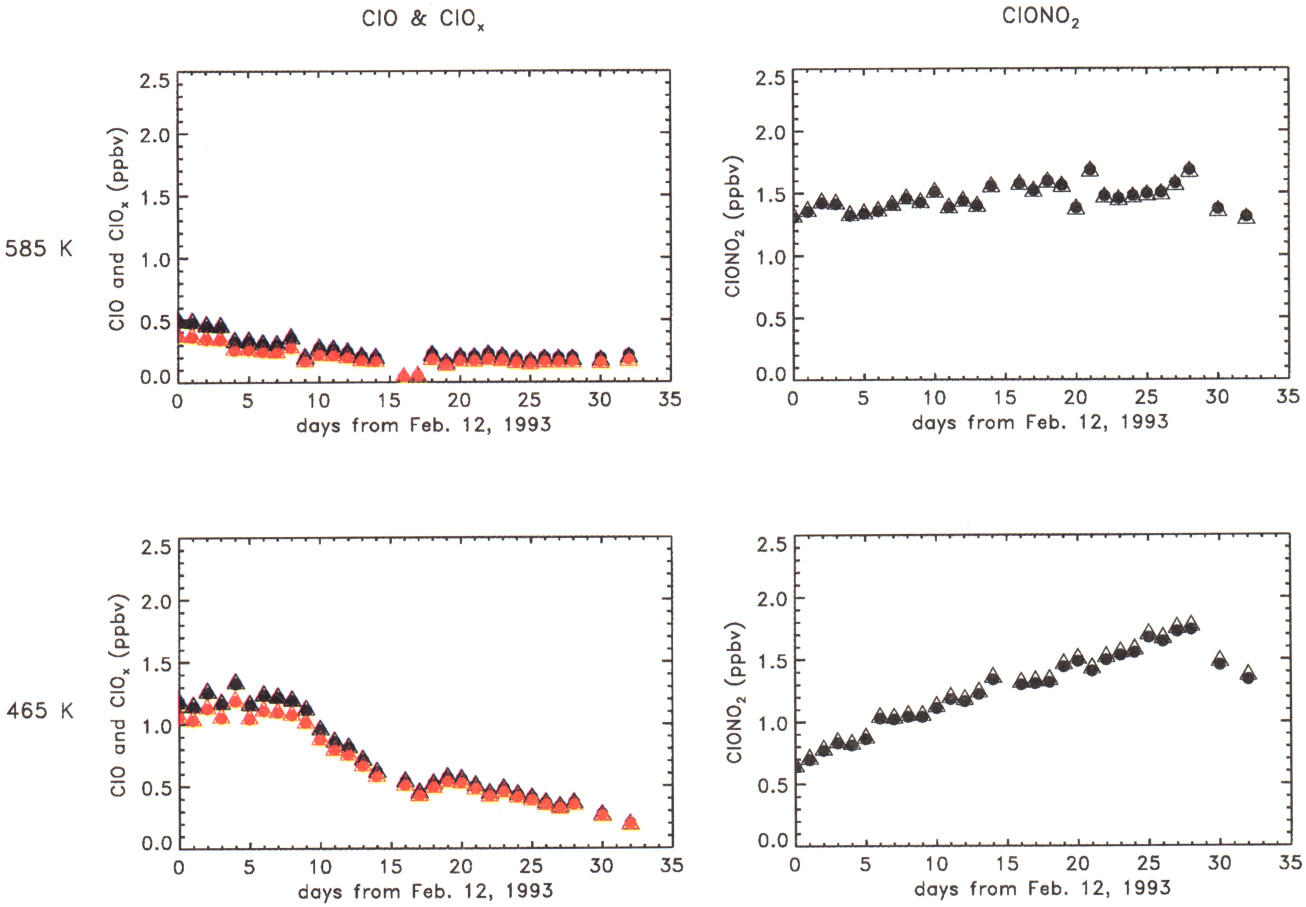

Plate 13. As in Plate 6 for the 1992–1993 northern hemisphere late-winter north-looking period.

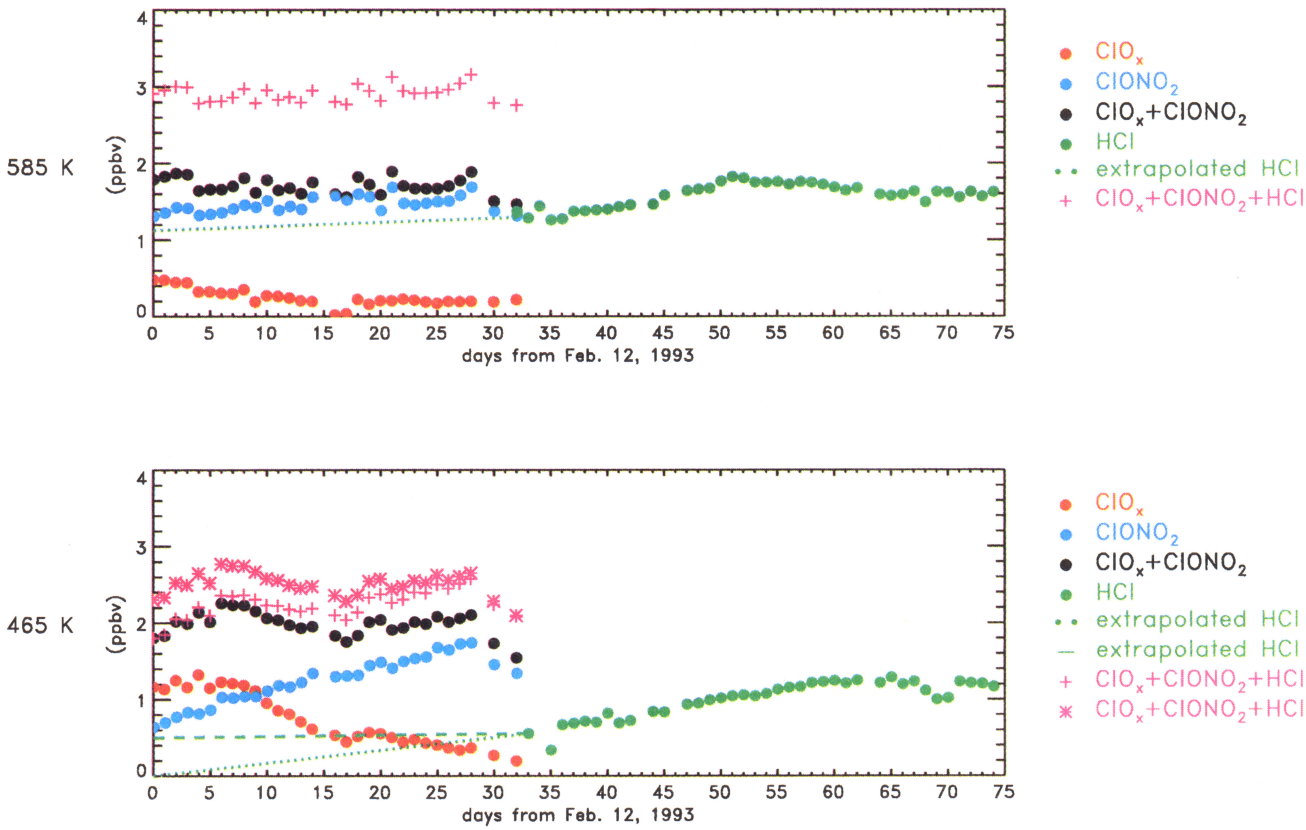

Plate 14. As in Plate 8 for the northern hemisphere. Note that at 585 K, the HCl is extrapolated using the $\partial(\mathrm{HCl})/\partial t$ value from the multiple linear regression; the extrapolation is begun from the line fit to the data and, consequently, does not exactly coincide with the first data point (compare Figure 5). In contrast, at 465 K the fitted line is not used and the backward extrapolations (to zero, dotted green line; to 0.5 ppbv, dashed green line) proceed from the actual data point.

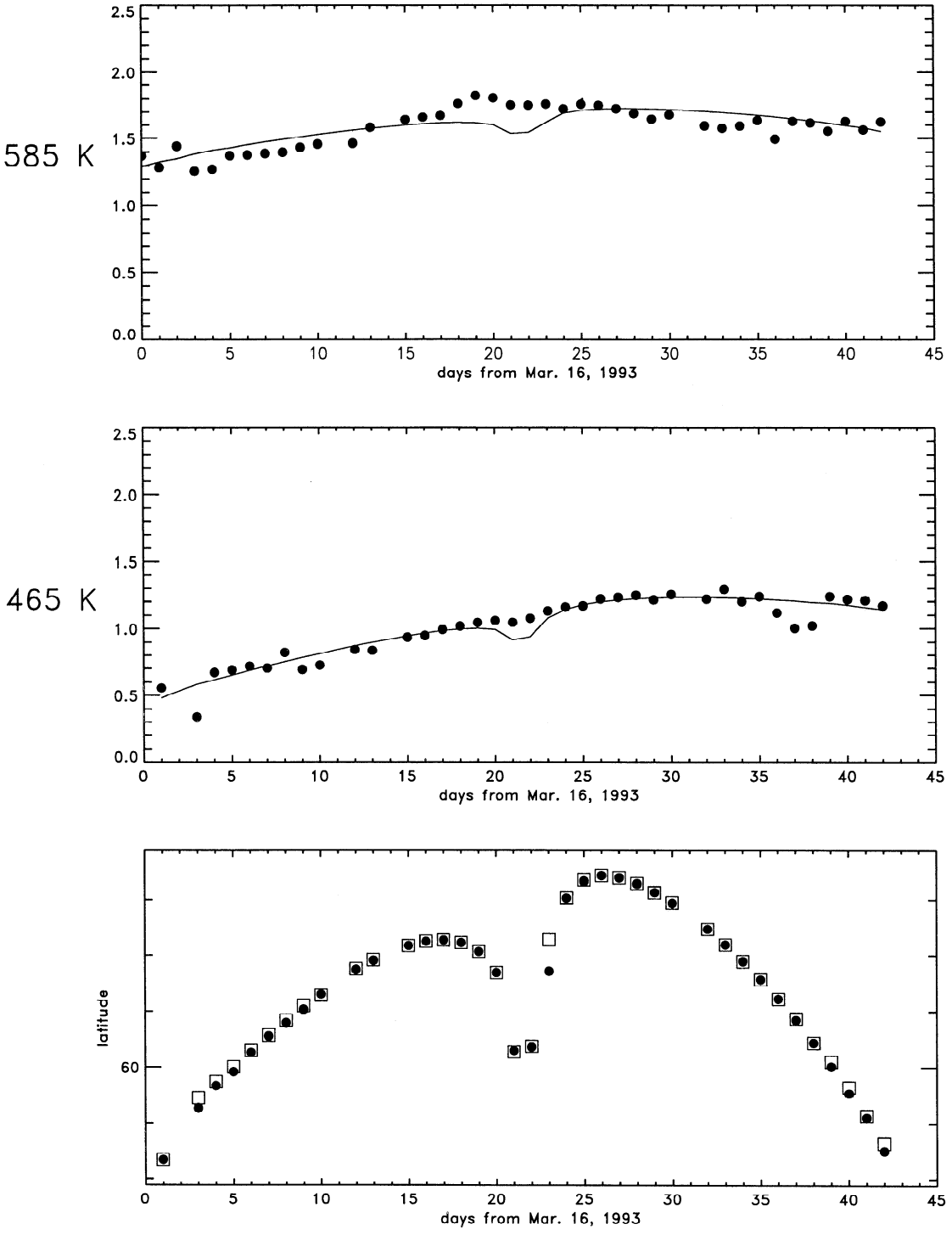

Figure 5. Time series, over the HALOE 1992–1993 northern vortex sampling period, of vortex-averaged (using the outermost PV contour; see text) mixing ratios of HALOE HCl (ppbv; solid circles) at 585 K (top) and 465 K (middle). Also shown (bottom) are the associated daily average latitudes of the profiles (open squares, 465 K; solid circles, 585 K). HALOE data are strong functions of both latitude and time, and multiple linear regression is used to fit curves (solid lines) to the daily averages at both levels.

very slight decrease in ClO_x + $ClONO_2$ + HCl (which varies around 2.5 ppbv). Thus there is approximate balance in the chlorine budget at both levels in the northern hemisphere.

4.4. Discussion

Manney et al. [1994c] show that the 1992–1993 Arctic lower stratospheric vortex is anomalously strong, isolated, and persistent, and is characterized by below-

average temperatures. It is thus more "Antarctic-like" than is typical. Despite these circumstances, both ground-based [*Notholt*, 1994] and aircraft measurements [*Blom et al.*, 1995] suggest no appreciable denitrification. Using UARS MLS data, *Santee et al.* [1995] find the observed depletion of gas-phase HNO_3 to be considerably smaller than that over Antarctica. Therefore, although the 1992–1993 winter represents fairly extreme Arctic conditions, gas-phase HNO_3 is nevertheless present in sufficient quantity to supply NO_2 for the rapid formation of $ClONO_2$. In contrast to the southern hemisphere, we find that the observed late-winter decrease in ClO_x is balanced by a corresponding increase in $ClONO_2$ at both 585 K and 465 K. This conclusion is in good agreement with the results from the AASE, AASE II, and EASOE campaigns outlined in section 1.

5. Summary

We have investigated the recovery of the perturbed chlorine chemistry in the lower stratospheric polar regions of both hemispheres. We have correlated MLS measurements of ClO and inferred ClO_x with simultaneous and colocated CLAES measurements of $ClONO_2$. Time series of vortex-averaged mixing ratios at both 585 K and 465 K have been analyzed for approximately month-long intervals during late winter: August 17 – September 17, 1992, in the southern hemisphere and February 12 – March 16, 1993, in the northern hemisphere. The magnitude of the diabatic descent at each level has been estimated from CLAES measurements of CH_4 and N_2O and used to adjust the observed mixing ratios for the effects of vertical transport.

In the southern hemisphere, continuing polar stratospheric cloud activity, as evidenced by CLAES measurements of aerosol extinction coefficient, prevented ClO from undergoing sustained decline until the latter half of the study period. Even after the enhanced ClO abundances started to recede, there was no significant chemical change seen in $ClONO_2$ at 465 K, and the $ClONO_2$ at 585 K was observed to decrease. Denitrification is expected to have inhibited the formation of $ClONO_2$ by removing gas-phase HNO_3, the source of NO_2. The observational results have also been compared to those from the SLIMCAT isentropic-coordinate chemical transport model [*Chipperfield et al.*, this issue], which was initialized with UARS data. The model reproduces the MLS ClO abundances and downward trend at 585 K, but underestimates MLS ClO by as much as 0.4 ppbv at 465 K. The model also reproduces CLAES $ClONO_2$ fairly well at 585 K, but underestimates it by as much as 0.6 ppbv at 465 K. Inclusion of the $OH + ClO \rightarrow HCl + O_2$ reaction as an 8% channel in the model suppresses the recovery of $ClONO_2$ (for the time period considered here) and promotes the conversion of ClO to HCl at both 585 K and 465 K. HALOE measurements of HCl in the southern polar vortex, obtained shortly after the MLS and CLAES data, were linearly extrapolated back to the time frame of the study period. At 585 K, the trend in inferred $ClO_x + ClONO_2 + HCl$ was found to be highly sensitive to the value to which the HCl was extrapolated on the first day of the interval, and the chlorine budget could be made to balance by setting HCl=0.6 ppbv on that day (September 3). At 465 K, although the addition of extrapolated HCl did improve the chlorine balance slightly, the contribution from calculated HCl was not sufficient to offset the observed losses, and an imbalance was found between the decrease in reactive chlorine and the change in the chlorine reservoirs. The difficulty in closing the chlorine budget at 465 K in the southern hemisphere may have arisen from complications caused by ongoing activation, incomplete photochemical assumptions, and/or inadequate data quality.

In the northern hemisphere, ClO was not so uniformly enhanced within the vortex as was observed over Antarctica. In addition, ClO appeared to diminish more rapidly at both levels in the northern hemisphere. Although the 1992–1993 Arctic lower stratospheric vortex was more "Antarctic-like" than is typical, sufficient gas-phase HNO_3 remained to supply NO_2 for the rapid formation of $ClONO_2$. In contrast to the southern hemisphere, the decrease in ClO_x at the end of winter was balanced at both 585 K and 465 K by a corresponding increase in $ClONO_2$. We found that $ClONO_2$ was the primary reservoir during recovery in the northern hemisphere, in good agreement with the results from previous Arctic studies.

Acknowledgments. The authors would like to thank our UARS colleagues for their support and their contributions to its success. We are grateful to National Meteorological Center (NMC) Climate Analysis Center personnel, especially M. E. Gelman and A. J. Miller, for making NMC data available to the UARS project. We would also like to thank T. Lungu for providing ClO data from the preliminary Version 4 retrieval algorithms, R. P. Thurstans and B. P. Ridenoure for graphics assistance, and T. Luu and L. Nakamura for data management. Helpful discussions with M. Allen, P. S. Connell, D. E. Kinnison, G. C. Toon, and R. Müller were greatly appreciated. M. L. Santee gratefully acknowledges support from the Resident Research Associateship program of the National Research Council. The work at the Jet Propulsion Laboratory, California Institute of Technology was sponsored by the National Aeronautics and Space Administration and the National Research Council, and the work at Cambridge University forms part of the UK Universities' Global Atmospheric Modelling Programme.

References

Adrian, G. P., et al., First results of ground-based FTIR measurements of atmospheric trace gases in North Sweden and Greenland during EASOE, *Geophys. Res. Lett.*, *21*, 1343 1346, 1994.

Anderson, J. G., W. H. Brune, and M. H. Proffitt, Ozone destruction by chlorine radicals within the Antarctic vortex: The spatial and temporal evolution of ClO-O_3 anticorrelation based on in situ ER-2 data, *J. Geophys. Res.*, *94*, 11,465–11,479, 1989.

Anderson, J. G., D. W. Toohey, and W. H. Brune, Free radicals within the Antarctic vortex: The role of CFCs in Antarctic ozone loss, *Science*, *251*, 39–46, 1991.

Andrews, D. G., Some comparisons between the middle at-

mosphere dynamics of the southern and northern hemispheres, *Pure Appl. Geophys., 130*, 213–232, 1989.

Arnold, F., and S. Spreng, Balloon-borne mass spectrometer measurements of HCl and HF in the winter Arctic stratosphere, *Geophys. Res. Lett., 21*, 1255–1258, 1994.

Barath, F. T., et al., The Upper Atmosphere Research Satellite Microwave Limb Sounder instrument, *J. Geophys. Res., 98*, 10,751–10,762, 1993.

Bell, W., N. A. Martin, T. D. Gardiner, N. R. Swann, P. T. Woods, P. F. Fogal, and J. W. Waters, Column measurements of stratospheric trace species over Åre, Sweden, in the winter of 1991–1992, *Geophys. Res. Lett., 21*, 1347–1350, 1994.

Blom, C. E., H. Fischer, N. Glatthor, T. Gulde, M. Höpfner, and C. Piesch, Spatial and temporal variability of $ClONO_2$, HNO_3, and O_3 in the Arctic winter of 1992/1993 as obtained by airborne infrared emission spectroscopy, *J. Geophys. Res., 100*, 9101–9114, 1995.

Braathen, G. O., M. Rummukainen, E. Kyrö, U. Schmidt, A. Dahlback, T. S. Jorgensen, R. Fabian, V. Rudakov, M. Gil, and R. Borchers, Temporal development of ozone within the Arctic vortex during the winter of 1991/92, *Geophys. Res. Lett., 21*, 1407–1410, 1994.

Brune, W. H., J. G. Anderson, and K. R. Chan, In situ observations of ClO in the Antarctic: ER-2 aircraft results from 54°S to 72°S latitude, *J. Geophys. Res., 94*, 16,649–16,663, 1989.

Brune, W. H., J. G. Anderson, D. W. Toohey, D. W. Fahey, S. R. Kawa, R. L. Jones, D. S. McKenna, and L. R. Poole, The potential for ozone depletion in the Arctic polar stratosphere, *Science, 252*, 1260–1266, 1991.

Chandra, S., C. H. Jackman, A. R. Douglass, E. L. Fleming, and D. B. Considine, Chlorine catalyzed destruction of ozone: Implications for ozone variability in the upper stratosphere, *Geophys. Res. Lett., 20*, 351–354, 1993.

Chipperfield, M. P., J. A. Pyle, C. E. Blom, N. Glatthor, M. Höpfner, T. Gulde, C. Piesch, and P. Simon, The variability of $ClONO_2$ and HNO_3 in the Arctic polar vortex: Comparison of Transall Michelson interferometer for passive atmospheric sounding measurements and three-dimensional model results, *J. Geophys. Res., 100*, 9115–9129, 1995.

Chipperfield, M. P., M. L. Santee, L. Froidevaux, G. L. Manney, W. G. Read, J. W. Waters, A. E. Roche, and J. M. Russell, Analysis of UARS data in the southern polar vortex in September 1992 using a chemical transport model, *J. Geophys. Res.*, this issue.

Coffey, M. T., W. G. Mankin, and A. Goldman, Airborne measurements of stratospheric constituents over Antarctica in the austral spring 1987, 2, Halogen and nitrogen trace species, *J. Geophys. Res., 94*, 16,597–16,613, 1989.

Collins, J. E., G. W. Sachse, B. E. Anderson, A. J. Weinheimer, J. G. Walega, and B. A. Ridley, AASE II in-situ tracer correlations of methane, nitrous oxide, and ozone as observed aboard the DC-8, *Geophys. Res. Lett., 20*, 2543–2546, 1993.

Crutzen, P. J., R. Müller, C. Brühl, and T. Peter, On the potential importance of the gas phase reaction $CH_3O_2 + ClO \rightarrow ClOO + CH_3O$ and the heterogeneous reaction $HOCl + HCl \rightarrow H_2O + Cl_2$ in "ozone hole" chemistry, *Geophys. Res. Lett., 19*, 1113–1116, 1992.

DeMore, W. B., S. P. Sander, D. M. Golden, R. F. Hampson, M. J. Kurylo, C. J. Howard, A. R. Ravishankara, C. E. Kolb, and M. J. Molina, *Chemical kinetics and photochemical data for use in stratospheric modeling, in Evaluation 11, JPL Publ. 94-26*, Jet Propul. Lab., Pasadena, Calif., 1994.

Dessler, A. E., D. B. Considine, G. A. Morris, M. R. Schoeberl, A. E. Roche, J. M. Russell, J. W. Waters, G. K. Yue, Correlated observations of HCl and $ClONO_2$ from UARS and implications for stratospheric chlorine partitioning, *Geophys. Res. Lett., 22*, 1721–1724, 1995.

de Zafra, R. L., M. Jaramillo, A. Parrish, P. Solomon, B. Connor, and J. Barrett, High concentrations of chlorine monoxide at low altitudes in the Antarctic spring stratosphere: Diurnal variation, *Nature, 328*, 408–411, 1987.

Douglass, A. R., M. R. Schoeberl, R. S. Stolarski, J. W. Waters, J. M. Russell III, A. E. Roche, and S. T. Massie, Interhemispheric differences in springtime production of HCl and $ClONO_2$ in the polar vortices, *J. Geophys. Res., 100*, 13,967–13,978, 1995.

Eckman, R. S., W. L. Grose, R. E. Turner, W. T. Blackshear, J. M. Russell III, L. Froidevaux, J. W. Waters, J. B. Kumer, and A. E. Roche, Stratospheric trace constituents simulated by a three-dimensional general circulation model: Comparison with UARS data, *J. Geophys. Res., 100*, 13,951–13,966, 1995.

Evans, W. F. J., Ozone depletion in the Arctic vortex at Alert during February 1989, *Geophys. Res. Lett., 17*, 167–170, 1990.

Fahey, D. W., D. M. Murphy, K. K. Kelly, M. K. W. Ko, M. H. Proffitt, C. S. Eubank, G. V. Ferry, M. Loewenstein, and K. R. Chan, Measurements of nitric oxide and total reactive nitrogen in the Antarctic stratosphere: Observations and chemical implications, *J. Geophys. Res., 94*, 16,665–16,681, 1989.

Farmer, C. B., G. C. Toon, P. W. Schaper, J.-F. Blavier, and L. L. Lowes, Stratospheric trace gases in the spring 1986 Antarctic atmosphere, *Nature, 329*, 126–130, 1987.

Gunson, M. R., M. C. Abrams, L. L. Lowes, E. Mahieu, R. Zander, C. P. Rinsland , M. K. W. Ko, N. D. Sze, and D. K. Weisenstein, Increase in levels of stratospheric chlorine and flourine loading between 1985 and 1992, *Geophys. Res. Lett., 21*, 2223–2226, 1994.

Hofmann, D. J., and T. Deshler, Evidence from balloon measurements for chemical depletion of stratospheric ozone in the Arctic winter of 1989–90, *Nature, 349*, 300–305, 1991.

Hofmann, D. J., T. Deshler, P. Aimedieu, W. A. Matthews, P. V. Johnston, Y. Kondo, W. R. Sheldon, G. J. Byrne, and J. R. Benbrook, Stratospheric clouds and ozone depletion in the Arctic during January 1989, *Nature, 340*, 117–121, 1989.

Jones, R. L., et al., Lagrangian photochemical modeling studies of the 1987 Antarctic spring vortex, 1, Comparison with AAOE observations, *J. Geophys. Res., 94*, 11,529–11,558, 1989.

Jones, R. L., D. S. McKenna, L. R. Poole, and S. Solomon, On the influence of polar stratospheric cloud formation on chemical composition during the 1988/89 Arctic winter, *Geophys. Res. Lett., 17*, 545–548, 1990.

Kawa, S. R., D. W. Fahey, L. C. Anderson, M. Loewenstein, and K. R. Chan, Measurements of total reactive nitrogen during the Airborne Arctic Stratospheric Experiment, *Geophys. Res. Lett., 17*, 485–488, 1990.

Kawa, S. R., D. W. Fahey, L. E. Heidt, W. H. Pollock, S. Solomon, D. E. Anderson, M. Loewenstein, M. H. Proffitt, J. J. Margitan, and K. R. Chan, Photochemical partitioning of the reactive nitrogen and chlorine reservoirs in the high-latitude stratosphere, *J. Geophys. Res., 97*, 7905–7923, 1992.

Kumer, J. B., J. L. Mergenthaler, and A. E. Roche, CLAES CH_4, N_2O, and CCL_2F_2 (F12) global data, *Geophys. Res. Lett., 20*, 1239–1242, 1993.

Kyrö, E., et al., Analysis of the ozone soundings made during the first quarter of 1989 in the Arctic, *J. Geophys. Res., 97*, 8083–8091, 1992.

Lary, D. J., M. P. Chipperfield, and R. Toumi, The potential

impact of the reaction OH + ClO → HCl + O_2 on polar ozone photochemistry, *J. Atmos. Chem.*, *21*, 61–79, 1995.

Liu, X., R. D. Blatherwick, F. J. Murcray, J. G. Keys, and S. Solomon, Measurements and model calculations of HCl column amounts and related parameters over McMurdo during the austral spring in 1989, *J. Geophys. Res.*, *97*, 20,795–20,804, 1992.

Loewenstein, M., J. R. Podolske, K. R. Chan, and S. E. Strahan, Nitrous oxide as a dynamical tracer in the 1987 Airborne Antarctic Ozone Experiment, *J. Geophys. Res.*, *94*, 11,589–11,598, 1989.

Loewenstein, M., J. R. Podolske, K. R. Chan, and S. E. Strahan, N_2O as a dynamical tracer in the Arctic vortex, *Geophys. Res. Lett.*, *17*, 477–480, 1990.

Lutman, E. R., R. Toumi, R. L. Jones, D. J. Lary, and J. A. Pyle, Box model studies of ClO_x deactivation and ozone loss during the 1991/92 northern hemisphere winter, *Geophys. Res. Lett.*, *21*, 1415–1418, 1994.

MacKenzie, I. A., R. S. Harwood, L. Froidevaux, W. G. Read, and J. W. Waters, Chemical loss of polar vortex ozone inferred from UARS MLS measurements of ClO during the Arctic and Antarctic late winters of 1993, *J. Geophys. Res.*, in press, 1996.

Mankin, W. G., M. T. Coffey, A. Goldman, M. R. Schoeberl, L. R. Lait, and P. A. Newman, Airborne measurements of stratospheric constituents over the Arctic in the winter of 1989, *Geophys. Res. Lett.*, *17*, 473–476, 1990.

Manney, G. L., and R. W. Zurek, Interhemispheric comparison of the development of the stratospheric polar vortex during fall: A 3-dimensional perspective for 1991–1992, *Geophys. Res. Lett.*, *20*, 1275–1278, 1993.

Manney, G. L., L. Froidevaux, J. W. Waters, L. S. Elson, E. F. Fishbein, R. W. Zurek, R. S. Harwood, and W. A. Lahoz, The evolution of ozone observed by UARS MLS in the 1992 late winter southern polar vortex, *Geophys. Res. Lett.*, *20*, 1279–1282, 1993.

Manney, G. L., et al., Chemical depletion of ozone in the Arctic lower stratosphere during winter 1992 93, *Nature*, *370*, 429–434, 1994a.

Manney, G. L., R. W. Zurek, A. O'Neill, and R. Swinbank, On the motion of air through the stratospheric polar vortex, *J. Atmos. Sci.*, *51*, 2973–2994, 1994b.

Manney, G. L., R. W. Zurek, M. E. Gelman, A. J. Miller, and R. Nagatani, The anomalous Arctic lower stratospheric polar vortex of 1992–1993, *Geophys. Res. Lett.*, *21*, 2405–2408, 1994c.

Massie, S. T., et al., Validation studies using multiwavelength Cryogenic Limb Array Etalon Spectrometer observations of stratospheric aerosol, *J. Geophys. Res.*, *101*, 9757–9773, 1996.

McCormick, M. P., C. R. Trepte and M. C. Pitts, Persistence of polar stratospheric clouds in the southern polar region, *J. Geophys. Res.*, *94*, 11,241–11,251, 1989.

McElroy, M. B., and R. J. Salawitch, Changing composition of the global stratosphere, *Science*, *243*, 763–770, 1989.

McKenna, D. S., R. L. Jones, L. R. Poole, S. Solomon, D. W. Fahey, K. K. Kelly, M. H. Proffitt, W. H. Brune, M. Loewenstein, and K. R. Chan, Calculations of ozone destruction during the 1988/89 Arctic winter, *Geophys. Res. Lett.*, *17*, 553–556, 1990.

Mergenthaler, J. L., J. B. Kumer, and A. E. Roche, CLAES south-looking aerosol observations for 1992, *Geophys. Res. Lett.*, *20*, 1295–1298, 1993.

Mergenthaler, J. L., et al., Validation of CLAES $ClONO_2$ measurements, *J. Geophys. Res.*, *101*, 9603–9620, 1996.

Minschwaner, K., R. J. Salawitch, and M. B. McElroy, Absorption of solar radiation by O_2: Implications for O_3 and lifetimes of N_2O, $CFCl_3$, and CF_2Cl_2, *J. Geophys. Res.*, *98*, 10,543–10,561, 1993.

Molina, L. T., and M. J. Molina, Production of Cl_2O_2 from the self-reaction of the ClO radical, *J. Phys. Chem.*, *91*, 433–436, 1987.

Müller, R., T. Peter, P. J. Crutzen, H. Oelhaf, G. P. Adrian, T. v. Clarmann, A. Wegner, U. Schmidt, and D. Lary, Chlorine chemistry and the potential for ozone depletion in the Arctic stratosphere in the winter of 1991/92, *Geophys. Res. Lett.*, *21*, 1427–1430, 1994.

Natarajan, M., and L. B. Callis, Stratospheric photochemical studies with atmospheric trace molecule spectroscopy (ATMOS) measurements, *J. Geophys. Res.*, *96*, 9361–9370, 1991.

Notholt, J., The Moon as a light source for FTIR measurements of stratospheric trace gases during the polar night: Application for HNO_3 in the Arctic, *J. Geophys. Res.*, *99*, 3607–3614, 1994.

Oelhaf, H., T. v. Clarmann, H. Fischer, F. Friedl-Vallon, C. Fritzsche, A. Linden, C. Piesch, M. Seefeldner, and W. Völker, Stratospheric $ClONO_2$ and HNO_3 profiles inside the Arctic vortex from MIPAS-B limb emission spectra obtained during EASOE, *Geophys. Res. Lett.*, *21*, 1263–1266, 1994.

Poole, L. R., and M. C. Pitts, Polar stratospheric cloud climatology based on Stratospheric Aerosol Measurement II observations from 1978 to 1989, *J. Geophys. Res.*, *99*, 13,083–13,089, 1994.

Prather, M., and A. H. Jaffe, Global impact of the Antarctic ozone hole: Chemical propagation, *J. Geophys. Res.*, *95*, 3473–3492, 1990.

Roche, A. E., J. B. Kumer, J. L. Mergenthaler, G. A. Ely, W. G. Uplinger, J. F. Potter, T. C. James, and L. W. Sterritt, The Cryogenic Limb Array Etalon Spectrometer (CLAES) on UARS: Experiment description and performance, *J. Geophys. Res.*, *98*, 10,763–10,775, 1993a.

Roche, A. E., J. B. Kumer, and J. L. Mergenthaler, CLAES observations of $ClONO_2$ and HNO_3 in the Antarctic stratosphere, between June 15 and September 17, 1992, *Geophys. Res. Lett.*, *20*, 1223–1226, 1993b.

Roche, A. E., J. B. Kumer, J. L. Mergenthaler, R. W. Nightingale, W. G. Uplinger, G. A. Ely, J. F. Potter, D. J. Wuebbles, P. S. Connell, and D. E. Kinnison, Observations of lower-stratospheric $ClONO_2$, HNO_3, and aerosol by the UARS CLAES experiment between January 1992 and April 1993, *J. Atmos. Sci.*, *51*, 2877–2902, 1994.

Roche, A. E., et al., Validation of CH_4 and N_2O measurements by the cryogenic limb array etalon spectrometer instrument on the Upper Atmosphere Research Satellite, *J. Geophys. Res.*, *101*, 9679–9710, 1996.

Rodriguez, J. M., et al., Nitrogen and chlorine species in the spring Antarctic stratosphere: Comparison of models with Airborne Antarctic Ozone Experiment observations, *J. Geophys. Res.*, *94*, 16,683–16,703, 1989.

Rosenfield, J. E., P. A. Newman, and M. R. Schoeberl, Computations of diabatic descent in the stratospheric polar vortex, *J. Geophys. Res.*, *99*, 16,677–16,689, 1994.

Russell, J. M., III, L. L. Gordley, J. H. Park, S. R. Drayson, W. D. Hesketh, R. J. Cicerone, A. F. Tuck, J. E. Frederick, J. E. Harries, and P. J. Crutzen, The Halogen Occultation Experiment, *J. Geophys. Res.*, *98*, 10,777–10,797, 1993.

Russell, J. M., III, et al., Validation of hydrogen chloride measurements made by the Halogen Occultation Experiment from the UARS platform, *J. Geophys. Res.*, *101*, 10,151–10,162, 1996.

Salawitch, R. J., et al., Loss of ozone in the Arctic vortex for the winter of 1989, *Geophys. Res. Lett.*, *17*, 561–564, 1990.

Salawitch, R. J., et al., Chemical loss of ozone in the Arctic polar vortex in the winter of 1991–1992, *Science*, *261*, 1146–1149, 1993.

Sander, S. P., R. R. Friedl, and Y. L. Yung, Rate of formation of the ClO Cl_2O_2 in the polar stratosphere: Implications for ozone loss, *Science*, *245*, 1095–1098, 1989.

Santee, M. L., W. G. Read, J. W. Waters, L. Froidevaux, G. L. Manney, D. A. Flower, R. F. Jarnot, R. S. Harwood, and G. E. Peckham, Interhemispheric differences in polar stratospheric HNO_3, H_2O, ClO, and O_3, *Science*, *267*, 849–852, 1995.

Schoeberl, M. R., and D. L. Hartmann, The dynamics of the stratospheric polar vortex and its relation to springtime ozone depletions, *Science*, *251*, 46–52, 1991.

Schoeberl, M. R., M. H. Proffitt, K. K. Kelly, L. R. Lait, P. A. Newman, J. E. Rosenfield, M. Loewenstein, J. R. Podolske, S. E. Strahan, and K. R. Chan, Stratospheric constituent trends from ER-2 profile data, *Geophys. Res. Lett.*, *17*, 469–472, 1990.

Schoeberl, M. R., L. R. Lait, P. A. Newman, and J. E. Rosenfield, The structure of the polar vortex, *J. Geophys. Res.*, *97*, 7859–7882, 1992.

Schoeberl, M. R., et al., The evolution of ClO and NO along air parcel trajectories, *Geophys. Res. Lett.*, *20*, 2511–2514, 1993.

Schoeberl, M. R., M. Luo, and J. E. Rosenfield, An analysis of the Antarctic Halogen Occultation Experiment trace gas observations, *J. Geophys. Res.*, *100*, 5159–5172, 1995.

Solomon, S., The mystery of the Antarctic ozone "hole", *Rev. Geophys.*, *26*, 131–148, 1988.

Solomon, S., Progress towards a quantitative understanding of Antarctic ozone depletion, *Nature*, *347*, 347–354, 1990.

Toohey, D. W., L. M. Avallone, L. R. Lait, P. A. Newman, M. R. Schoeberl, D. W. Fahey, E. L. Woodbridge, and J. G. Anderson, The seasonal evolution of reactive chlorine in the northern hemisphere stratosphere, *Science*, *261*, 1134–1136, 1993.

Toon, G. C., C. B. Farmer, L. L. Lowes, P. W. Schaper, J.-F. Blavier, and R. H. Norton, Infrared aircraft measurements of stratospheric composition over Antarctica during September 1987, *J. Geophys. Res.*, *94*, 16,571–16,596, 1989.

Toon, G. C., J.-F. Blavier, J. N. Solario, and J. T. Szeto, Airborne observations of the 1992 Arctic winter stratosphere by FTIR solar absorption spectroscopy, *SPIE*, *1715*, 457–467, 1992.

Toumi, R., and S. Bekki, The importance of the reactions between OH and ClO for stratospheric ozone, *Geophys. Res. Lett.*, *20*, 2447–2450, 1993.

Traub, W. A., K. W. Jucks, D. G. Johnson, and K. V. Chance, Chemical change in the Arctic vortex during AASE II, *Geophys. Res. Lett.*, *21*, 2595–2598, 1994.

Tuck, A. F., Synoptic and chemical evolution of the Antarctic vortex in late winter and early spring, 1987, *J. Geophys. Res.*, *94*, 11,687–11,737, 1989.

Tuck, A. F., et al., Polar stratospheric cloud processed air and potential vorticity in the northern hemisphere lower stratosphere at midlatitudes during winter, *J. Geophys. Res.*, *97*, 7883–7904, 1992.

Turco, R. P., O. B. Toon, and P. Hamill, Heterogeneous physicochemistry of the polar ozone hole, *J. Geophys. Res.*, *94*, 16,493–16,510, 1989.

Waters, J. W., Microwave limb sounding, in *Atmospheric Remote Sensing by Microwave Radiometry*, edited by M. A. Janssen, pp. 383–496, John Wiley, New York, 1993.

Waters, J. W., L. Froidevaux, W. G. Read, G. L. Manney, L. S. Elson, D. A. Flower, R. F. Jarnot, and R. S. Harwood, Stratospheric ClO and ozone from the Microwave Limb Sounder on the Upper Atmosphere Research Satellite, *Nature*, *362*, 597–602, 1993a.

Waters, J. W., L. Froidevaux, G. L. Manney, W. G. Read, and L. S. Elson, MLS Observations of lower stratospheric ClO and O_3 in the 1992 southern hemisphere winter, *Geophys. Res. Lett.*, *20*, 1219–1222, 1993b.

Waters, J. W., G. L. Manney, W. G. Read, L. Froidevaux, D. A. Flower, and R. F. Jarnot, UARS MLS observations of lower stratospheric ClO in the 1992–93 and 1993–94 Arctic winter vortices, *Geophys. Res. Lett.*, *22*, 823–826, 1995.

Waters, J. W., et al., Validation of UARS Microwave Limb Sounder ClO measurements, *J. Geophys. Res.*, *101*, 10,091–10,127, 1996.

Webster, C. R., R. D. May, D. W. Toohey, L. M. Avallone, J. G. Anderson, P. Newman, L. Lait, M. R. Schoeberl, J. W. Elkins, and K. R. Chan, Chlorine chemistry on polar stratospheric cloud particles in the Arctic winter, *Science*, *261*, 1130–1134, 1993.

Woodbridge, E. L., et al., Estimates of total organic and inorganic chlorine in the lower stratosphere from in situ and flask measurements during AASE II, *J. Geophys. Res.*, *100*, 3057–3064, 1995.

World Meteorological Organization (WMO), Scientific assessment of ozone depletion: 1994, *WMO Rep. 37*, Global Ozone Res. and Monit. Proj., Geneva, 1995.

M. P. Chipperfield, Department of Chemistry, University of Cambridge, UK.

L. Froidevaux, G. L. Manney, W. G. Read, M. L. Santee (corresponding author), and J. W. Waters, Jet Propulsion Laboratory, Mail Stop 183–701, 4800 Oak Grove Drive, Pasadena, CA 91109.

J. B. Kumer, J. L. Mergenthaler, and A. E. Roche, Lockheed Palo Alto Research Laboratory, 3251 Hanover St., Palo Alto, CA 94061.

J. M. Russell III, NASA Langley Research Center, Hampton, VA 23681.

(Received May 12, 1995; revised January 5, 1996;
accepted February 1, 1996.)